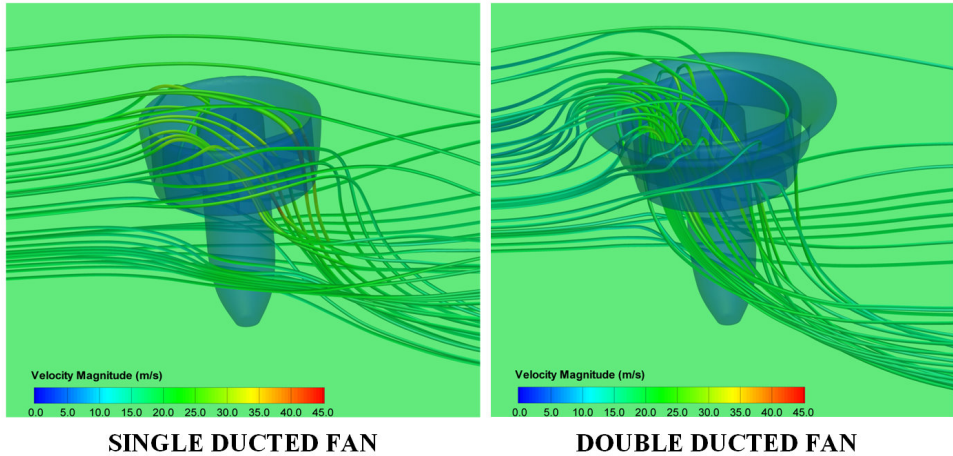


DOUBLE DUCTED FAN (DDF)



By

Cengiz CAMCI and Ali AKTURK

A technology description document

Turbomachinery Aero-heat Transfer Laboratory
Vertical Lift Research Center of Excellence
Department of Aerospace Engineering
The Pennsylvania State University



September 3, 2010

Abstract

This technical paper describes a novel ducted fan inlet flow conditioning concept that will significantly improve the performance and controllability of V/STOL ‘*vertical/short take off take-off and landing*’ UAVs ‘*uninhabited aerial vehicles*’ and many other ducted fan based systems. The new concept that will significantly reduce the inlet lip separation related performance penalties in the forward flight zone is named ‘*DOUBLE DUCTED FAN (DDF)*’. The current concept uses a secondary stationary duct system to control ‘*inlet lip separation*’ related momentum deficit at the inlet of the fan rotor occurring at elevated forward flight velocities. The DDF is self-adjusting in a wide forward flight velocity range. DDFs corrective aerodynamic influence becomes more pronounced with increasing flight velocity due to its inherent design properties. The DDF can also be implemented as a ‘*Variable Double Ducted Fan*’ (VDDF) for a much more effective inlet lip separation control in a wide range of horizontal flight velocities in UAVs, air vehicles, trains, buses, marine vehicles and any axial flow fan system where there is a local zone in which there are strong radial velocity components distorting the inlet flow. Most axial flow fans are designed for an inlet flow with zero or minimal inlet flow distortion. The DDF concept is proven to be an effective way of dealing with inlet flow distortions occurring near the lip section of any axial flow fan rotor system.

Contents

1	Introduction	4
1.1	Upstream Lip Region Flow Physics for Ducted Fans in Forward Flight	5
1.2	Past Studies of Ducted Fan Aerodynamics in Forward Flight	6
1.3	Lip Separation at High Angle of Attack	13
1.4	Adverse Effects of Upstream Lip Separation in Forward Flight	15
1.5	Patents Related to Ducted Fan Powered Vertical Lift Systems and Their Operation in Forward Flight	16
2	Double Ducted Fan (DDF) as a Novel Concept	26
2.1	Geometric Definition of DDF	27
2.2	Converging-Diverging Channel in the Duct	28
2.3	Various Possible Double Ducted Fan Geometries	30
3	Method of Analysis used in (DDF) Concept Development	32
3.1	Radial Equilibrium Based Analysis of Ducted Fan in Hover and Forward Flight	32
3.1.1	Computational Model Description	32
3.1.2	Boundary Conditions	33
3.1.3	Actuator Disk Model	36
4	DDF Concept Validation	39
4.1	Reference Ducted Fan Characteristics	39
4.2	Air Breathing Character of DDF in Forward Flight	41
4.3	A Comparative Evaluation of Local Velocity Magnitude, Stream- lines and Total Pressure for All Three Ducts	48
4.3.1	CASE-A Tall (DDF) versus Baseline Duct Results /at 10 m/s and 20 m/s	48

4.3.2	CASE-B Short (DDF) versus Baseline Duct Results at 10 m/s and 20 m/s	53
4.4	Upstream Lip Region Local Flow Improvements in (DDF)	57
4.4.1	Static Pressure Distribution around the Lip Section of the Baseline Duct	58
4.4.2	Static Pressure Distribution around the Lip section of the Double Ducted Fan (DDF)	59
4.4.3	Skin Friction Distribution around the Leading Edge of the Duct	60
5	Conclusions	62
	Bibliography	65

Nomenclature

β_1	Blade inlet angle (deg)
β_2	Blade exit angle (deg)
c	Chord length (m)
c_1	Rotor inlet absolute velocity (m/s)
c_2	Rotor exit absolute velocity (m/s)
c_θ	Tangential (swirl) component of the velocity (m/s)
c_x	Axial component of the velocity (m/s)
D	Overall diameter of the baseline ducted fan (m)
h	Rotor blade height (Rotor tip radius - Rotor hub radius)(m)
p	Static pressure (pa)
ρ	Density (kg/m ³)
ω	Rotational speed (radian/s)
r	Radial distance measured from origin (m)
t	Rotor tip clearance (m)
w_1	Rotor inlet relative velocity (m/s)
w_2	Rotor exit relative velocity (m/s)
X	Axial coordinate measured from the inlet plane of the standard duct (m)
x	$x = X/c$, non-dimensional axial distance

Chapter 1

Introduction

Although there is a strong interest in V/STOL UAV community to effectively deal with the upstream lip separation problem of ducted fans, the inlet flow distortion problem is common to many present day fan rotors in a wide variety of applications. The current conceptual design study clearly shows that the DDF approach is applicable to any axial flow fan unit in which there is an inlet flow distortion mainly because the inlet flow direction is not well aligned with the axis of rotation of the axial fan system. A few other examples that will easily benefit from the DDF concept described in this document are the cooling fans that are horizontally mounted at the roof of electric/diesel train locomotive propulsion cabins, air conditioning fans frequently installed at the roofs of passenger buses and cooling/utility fans that are flush mounted to external surfaces in marine vehicles.

Current approach for proving concept validity: A conventional baseline duct without any lip separation control feature is compared to two different double ducted fans named DDF-A and DDF-B via 3D, viscous and turbulent computational flow analysis. Both hover and forward flight conditions are considered. Significant relative improvements from DDF-A and DDF-B are in the areas of vertical force (thrust) enhancement, nose-up pitching moment control and recovery of mass flow rate in a wide horizontal flight range. The results show a major reduction of highly 3D and re-circulatory inlet lip separation zone when the DDF concept is implemented. The improved uniformity of fan exit flow and reduced differentials between the leading side and trailing side are obvious performance enhancing features of the novel concept. The local details of the flow near the entrance area of the leading side of the ducted fan are explained via detailed static

pressure distributions and skin friction coefficients obtained from 3D viscous and turbulent flow analysis including a simulated rotor in the duct. The current rotor flow energy addition simulation is via a radial equilibrium analysis which is a highly time efficient approach implemented into a RANS based flow model.

1.1 Upstream Lip Region Flow Physics for Ducted Fans in Forward Flight

Ducted fan systems horizontally moving at 90° angle of attack all inherently have an inlet flow direction that significantly deviates from the axis of the rotation. The inlet flow distortion near the leading side of all of these fan inlets becomes more problematic with increasing vehicle speed. The inlet flow distortion passing through a typical axial flow fan rotor becomes increasingly detrimental with elevated forward flight velocity. The lip separation occurring on the inner side of the lip section severely limits the lift generation and controllability of V/STOL UAVs. In general, the leading side of the fan near the lip separation zone breathes poorly when compared to the trailing side of the ducted fan. The trailing side total pressure is usually much higher than the total pressure observed near the leading side at the exit of the rotor. The flow near the leading side is adversely influenced by a separated flow zone that is characterized as highly re-circulatory, low momentum, unsteady and turbulent.

Conventional ducted fan systems also have a tip clearance loss that is proportional with the effective tip gap size inherent to each design. The specific shape of the tip platform and the surface properties and arrangement designed onto the casing surface also influences the magnitude of tip clearance loss. This aerodynamic deficiency is measured as a significant total pressure loss near the tip at the exit of the rotor all around the circumference when the vehicle is only hovering with no horizontal flight. When the vehicle transits into a horizontal flight, the total pressure loss/deficit at the exit of the rotor near the leading side is much more significant than “*hover only*” loss of the ducted fan. In addition to the conventional tip clearance energy loss, the rotor generates additional losses near the leading side, because of the re-circulatory low momentum fluid entering into the rotor near the tip section. This is clearly an off-design condition for an axial flow fan that is designed for a reasonably uniform inlet axial velocity profile in the spanwise

direction. The immediate results of any inlet flow distortion entering into an axial fan rotor in horizontal flight are the loss of rotor's energy addition capability to the fluid near the leading side, an imbalance of the local mass flow rate between the leading side and trailing side, an imbalance of the total pressure resulting at the rotor exit between the leading side and trailing side, a significant loss of lifting ability due to highly non-axisymmetric and unnecessarily 3D fan exit jet flow, unwanted nose-up pitching moment generation because the local static distributions imposed on the duct inner surfaces.

1.2 Past Studies of Ducted Fan Aerodynamics in Forward Flight

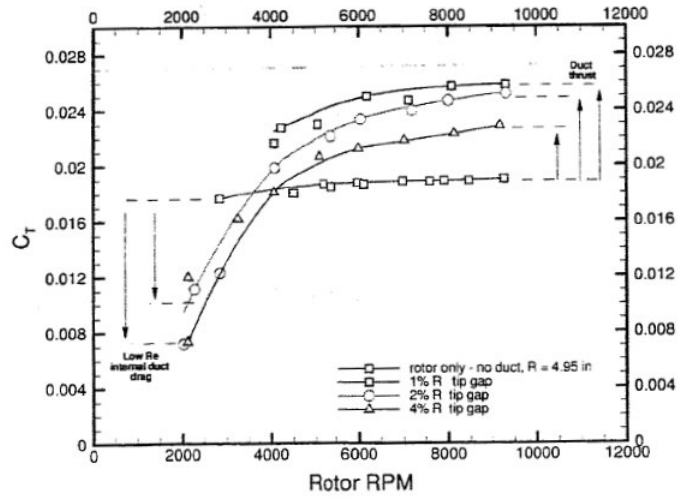
The viscous flow characteristics of the ducted fan are complex. These vehicles need to be capable of flight in a broad range of atmospheric conditions, including the complex turbulent flow fields around buildings and trees. When a V/STOL ducted fan is in horizontal flight, because of the relative inlet flow dominantly parallel to its inlet plane, problems related to flow separation at the leading edge duct lip are encountered. When the V/STOL vehicle is in perfect horizontal flight the angle between the relative inlet flow direction and the axis of rotation of the rotor is about 90° . This angle is usually termed as "*angle of attack*". At high angle of attack, the inlet flow separation leads to problems within the duct and may result in a high nose-up pitching moment as the forward speed is increased. Therefore, measuring and predicting the mean flow characteristics of ducted fans is crucial to understand the problems related to reliable and controllable horizontal flights. Numerous studies have been undertaken in order to quantify the flow field characteristics around ducted fans. The operation of an axial flow fan with strong inlet flow distortion severely affects the performance of the rotor especially near the tip region of the blades.

Experimental investigation has been the major approach to study the mean flow characteristics of the conventional ducted fan. Abrego and Buleaga [1] performed wind tunnel tests to determine the performance characteristics of ducted fans for axial and forward flight conditions. Their study resulted in showing important effect of exit vane flap deflection and flap chord length on providing side force.

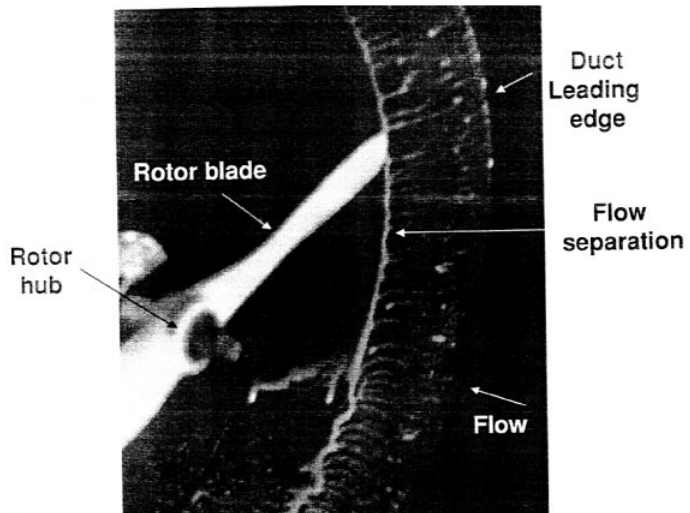
Martin and Tung [2] tested a ducted fan V/STOL UAV with a 10-inch diameter rotor. They measured aerodynamic loads on the vehicle for different angles of attack(from 0° to 110°) in hover and different crosswind velocities (41 knots, 70 ft/s). Both models were tested with fixed-pitch propellers of varying diameters, to test tip clearances from 1% to 4% (based on rotor tip radius). They also included hot-wire velocity surveys at inner and outer surface of the duct and across the downstream wake emphasizing the effect of tip gap on the thrust force produced. In addition, their study showed the effect of leading edge radius of the duct on the stall performance and stability of the vehicle. Figure 1.1 illustrates thrust of the system is decreasing with increasing tip gap height. Their results also showed that for lower rotational speeds open rotor thrust was higher than ducted fan thrust. They explained this by pointing out the increase in viscous losses inside the duct for low rotational speed operations. Figure 1.1b shows their oil flow visualization study. They have shown interaction of duct boundary layer and tip leakage vortex in their study.

Fleming *et al.*[3] published the results of a study on the performance performance of ducted fan inlet lips and exit vanes, in crosswind . Beside the experimental study they performed in wind tunnel, they also run computational analysis on Vertical Take-Off and Landing Unmanned Aerial Vehicles (VTOL UAV) ducted fans. Beside conventional control vanes, they tested seven different auxiliary control devices in crosswind. These control devices are an internal duct vane and thrust reverser that are adapted from Moller's control device [4], a "duct deflector" on the windward side of the internal duct wall; a trailing edge flap on the leeward side of the duct, which increases the effective camber of the duct profile; an inlet lip spoiler at the windward side; "*leading edge slat*" on the leeward side of the inlet; and lip flow control using normal and tangential flow blowing at the lip. Figure 1.3 shows control devices tested by Fleming *et al.*[3]. They have tested their 10 inch diameter ducted fan model in hover and crosswind up to 50 ft/s. They have selected "*lip flow control by blowing*", "*internal duct vane*" and "*internal duct deflector with bleed*" as efficiently performing devices. At low crosswind speeds, control vanes performed better than other methods. However, as the crosswind speed increased, the authors observed that the control vanes are stalled.

Graf *et al.*[5, 6] improved ducted fan forward flight performance with a recently designed leading edge geometry, which became a significant factor in offsetting the effects of adverse aerodynamic characteristics for elevated



(a)



(b)

Figure 1.1: (a) Thrust variation with rpm and tip gap(b) surface flow visualization of rotor induced separation in the tip path plane [2]

horizontal flight speeds. They have tested the effects of five different lip geometries. They have concluded that the duct lip shape is the most influential feature in offsetting the effects of the adverse aerodynamic characteristics. While a particular lip shape may perform well in hover conditions, its per-

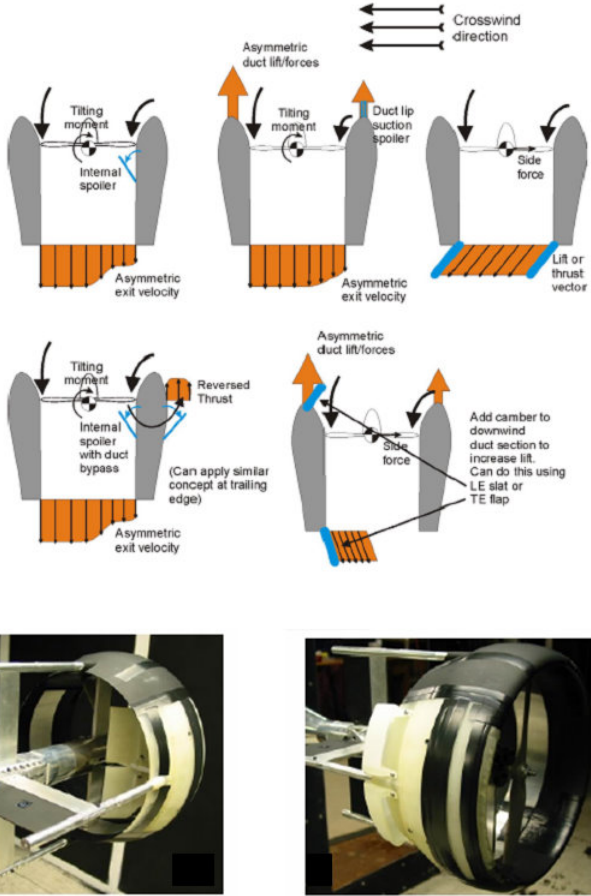


Figure 1.2: Control devices tested by Fleming *et al.*[3]

formance in crosswind conditions can be inferior to other designs.

Lazareff [7] investigated the aerodynamic performance of ducted fans by using both theoretical and experimental methods. The flight performance calculations are also shown in that study. The difference between ducted fans and free propellers is extensively discussed.

Weelden and Smith tried investigated ducted fan aerothermodynamic performance by utilizing systematic component build-up approach [8]. They emphasized the importance of the inlet and diffuser in performance of ducted fans.

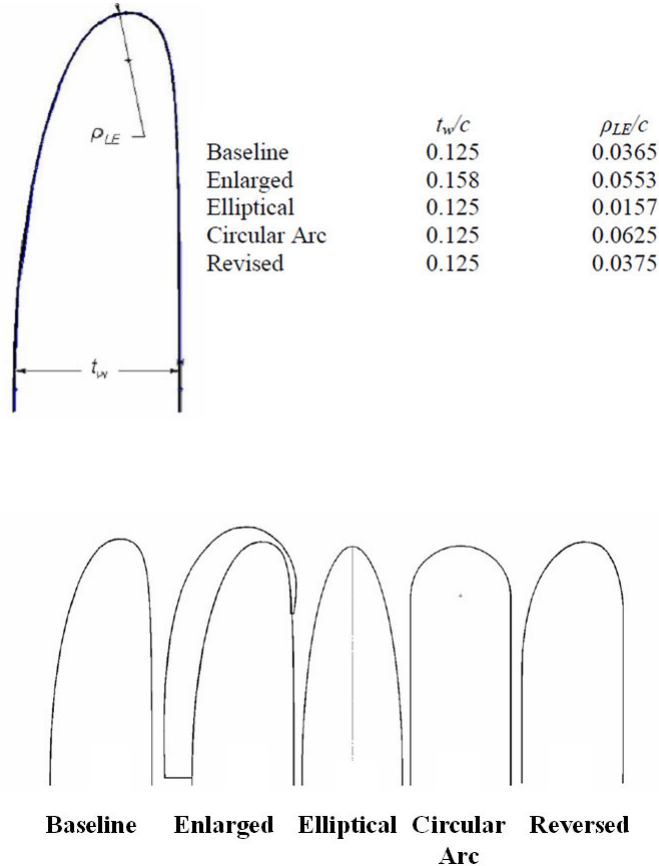


Figure 1.3: Tested inlet lip shapes Graf *et al.*[5, 6]

Kriebel and Mendenball also carried out a theoretical and experimental study to predict ducted fan performance [9]. They developed methods for predicting the forces and moments on the duct, duct surface pressure distributions and boundary-layer separation. They have compared their predictions with measurements made on the Bell X-22A and Doak VZ-4 aircraft models. Their model qualitatively predicted the force and moment, the pressure distribution , and the separation of the boundary layer over the entire operating range of propeller thrust and free-stream angle of attack.

Mort and Gamse [10] investigated aerodynamic characteristics of a seven foot diameter ducted propeller which was used on the Bell Aerosystems

Company X-22A airplane. They reported aerodynamic characteristics for variations of power, free-stream velocity, blade angle, and duct angle of attack. Stall of both the upstream and downstream duct lips of this seven foot diameter ducted fan was examined as a function of angle of attack. It was found that the onset of separation on the upstream lip will be encountered; however, complete separation on this lip will be encountered only during conditions of low power and high duct angle of attack.

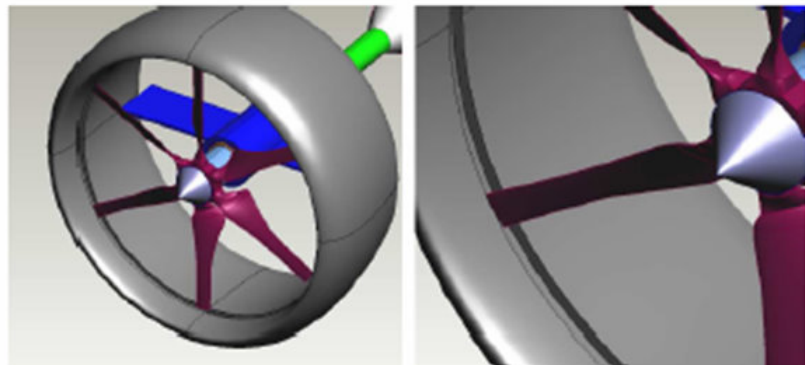
Mort and Yaggy [11, 12] performed hover and forward flight tests on a four foot diameter wing-tip mounted ducted fan that is used on Doak VZ-4-DA. Performance characteristics for the ducted fan were reported. They emphasized that pitching moment was rapidly changed and required power was increased due to separation, which occurred at windward side duct lip. They also reported that ducted fan supported by a fixed wing required less power in comparison to free flying ducted fan.

Weir has a study on experimental and theoretical performance of ducted fans with different inlet lip configurations [13]. In this study the moments and forces affecting the ducted fan were measured for different configurations. The design of exit vanes and fan rotor is also mentioned in the paper. The effect of the inlet lip radius on the lift and pitching moment combined with a diffuser is carefully investigated. As the inlet lip radius is increased the lift force of the ducted fan is also increased slightly. Adding a diffuser to the system has also positive effects on the lift. However, they both produce increased pitching moments.

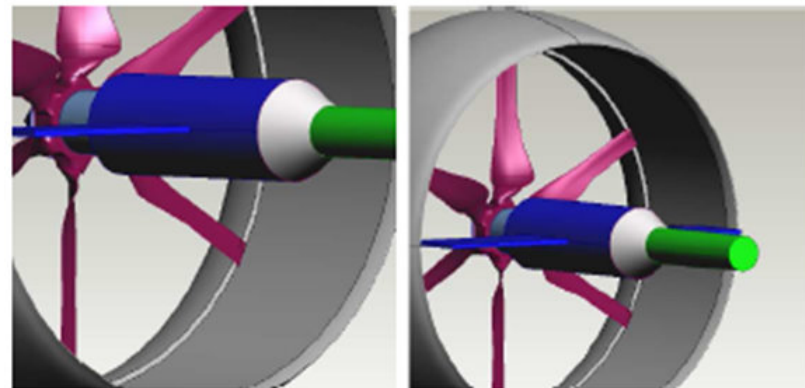
Pereira performed an experimental study on the effects of various shroud profile shapes on the performance of MAV-scale shrouded rotors [14]. Seventeen ducted fan models with a nominal rotor diameter of 16 cm (6.3 in) and various values of diffuser expansion angle, diffuser length, inlet lip radius and blade tip clearance were tested at various rotor collective angles. Tests performed for open rotor and a single shrouded-rotor model at a single collective in translational flight, at angles of attack from 0° (axial flow) to 90° (edgewise flow), and at various advance ratios are reported.

Martin and Boxwell [15] tested two ducted fan models that were designed to effectively eliminate the tip leakage. Both models were derived from the baseline (10-inch inner-diameter shroud) which is explained in their previous study [2]. In their first design, they have created a notch and fit the propeller inside the notch. In their second design, a rearward-facing step was cut into

the inner shroud. Their designs are shown in Figure 1.4. The computational analysis resulted in an increase in inlet lip suction and an increase in performance. However, the experimental thrust and power measurements, showed no difference in performance of these designs when compared to their baseline duct.



Notched duct



Rearward-facing stepped duct

Figure 1.4: Notched and stepped duct designs [15]

In addition to experimental studies, the ducted fan design and performance analyses were widely performed by using computational flow modeling. Lind *et al.*[16] carried out a computational study using a panel method. They compared their results to the experimental results from Martin and Tung [2]. He and Xin [17] developed the ducted fan models based on a non-uniform and unsteady ring vortex formulation. A numerical study in axial and horizontal flight conditions was conducted and validated with measured data. Chang *et al.*[18] developed an accurate grid generation methodology known as “*the curve adaptive option*” to model several industrial ducted fans. An axisymmetric, incompressible Navier-Stokes solver was implemented to calculate the flow field of a duct fan. The computational results agreed well with available wind tunnel data. Ahn *et al.*[19] applied a computational method to their ducted fan system to identify the design parameters which affect its performance. Their ducted fan system was designed by using the stream-surface based axisymmetric analysis which considered overall physical characteristics and design parameters of the system. Ko *et al.*[20] developed a computer code aimed at the preliminary design of a ducted fan system. This code was validated using data from many wind tunnel and flight tests. It was also extensively used in the design of commercial ducted fans. Recently, Zhao and Bil [21] proposed a CFD simulation to design and analyze an aerodynamic model of a ducted fan UAV in preliminary design phase with different speeds and angles of attacks.

1.3 Lip Separation at High Angle of Attack

The new concept named “*Double-Ducted Fan (DDF)*” is based on a very effective fluid mechanics scheme of reducing and controlling the upstream lip separation in a ducted fan operating at high angle of attack. Early research results clearly demonstrating the limits of onset of upstream lip separation as a function of angle of attack are summarized in Figure 1.5. A full scale duplicate of the V/STOL ducted propeller used on the Bell Aerosystems Co. X-22A airplane was tested in Ames Research center by Mort and Gamse [11, 12]. Stall of both the upstream and downstream duct lips of this seven foot diameter ducted fan was examined in function of angle of attack. The angle of attack of the ducted fan is the angle between the approaching flow direction and the axis of rotation of the rotor. It was found that the onset of separation on the upstream lip will be encountered; however, complete separation on this lip will be encountered only during

conditions of low power and high duct angle of attack corresponding to high rates of descent.

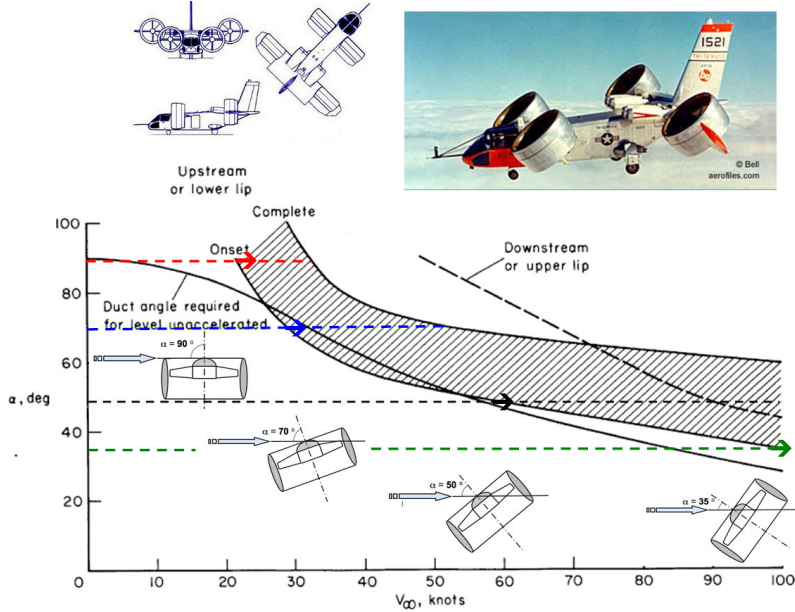


Figure 1.5: Upstream duct lip stall in function of angle of attack for X-22A ducted fan [11, 12]

Tests of a wing-tip-mounted 4-foot-diameter ducted fan were performed for a limited range of operating conditions by Mort and Yaggy [10]. At large duct angles of attack, the inside of the upstream duct lip stalled causing a rapid change in the duct pitching moments and accompanying increase in the power required. At low horizontal velocities this lip stall would probably limit the rate of descent of a vehicle with a wing tip mounted ducted fan. The wind tunnel test results shown in Figure 1.5 are highly relevant in demonstrating the beneficial aerodynamic characteristics of the double ducted fan DDF concept presented in this section.

Although, the reference ducted fan rotor had a tip clearance of $t/h=5.8\%$, the tip clearance influence on the rotor downstream flow was knowingly excluded from the current 3D computational flow effort. The present simplified rotor flow model does not include tip clearance effects since the current effort is focused on the accurate simulation of the lip separation flow during

forward flight of the vehicle. A radial equilibrium theory based rotor disk without a tip gap was chosen as a simplified and time efficient rotor model in this section.

1.4 Adverse Effects of Upstream Lip Separation in Forward Flight

At high angle of attack, the onset separation at the upstream duct lip is accompanied by the formation of a separation bubble. Existence of a significant separation bubble severely distorts inlet flow of the fan rotor especially near the leading side and in the tip clearance region. Distorted inlet flow causes an asymmetric loading of the ducted fan which increases the power required for level un-accelerated flight and noise level. The immediate results of operating a ducted fan in horizontal flight regime especially at high angle of attack are as follows:

- Increased aerodynamic losses and temporal instability of the fan rotor flow when “*inlet flow distortion*” from “*the lip separation area*” finds its way into the tip clearance gap leading to the loss of “*energy addition capability*” of the rotor.
- Reduced thrust generation from the upstream side of the duct due to the rotor breathing low-momentum and re-circulatory, turbulent flow.
- A severe imbalance of the duct inner static pressure field resulting from low momentum fluid entering into the rotor on the leading side and high momentum fluid unnecessarily energized near the trailing side of the rotor.
- A measurable increase in power demand and fuel consumption when the lip separation occurs to keep up with a given operational task.
- Lip separation and its interaction with the tip gap flow requires a much more complex vehicle control system because of the severe non-uniformity of the exit jet in circumferential direction and excessive nose-up pitching moment generation.
- At low horizontal speeds a severe limitation in the rate of descent and vehicle controllability may occur because of more pronounced lip

separation. Low power requirement of a typical descent results in a lower disk loading and more pronounced lip separation.

- Excessive noise and vibration from the rotor working with a significant inlet flow distortion.
- Very complex unsteady interactions of duct exit flow with control surfaces.

1.5 Patents Related to Ducted Fan Powered Vertical Lift Systems and Their Operation in Forward Flight

Ducted fans are very popular among the vertical lift systems. They have been used in many conceptually designed VTOL vehicles. Patents related to ducted fan powered vertical take-off vehicles are described in this section.

Dorman, 2,951,661 (1960): Four ducted fan/propeller units located on each quadrant of a square vehicle footprint are used as lift generating components to be used in a heavier than air VTOL vehicle, Dorman [22]. The axis of rotation of each ducted fan unit is normal to the horizontal plane. This is one of the earliest presentations of using ducted fans in VTOL vehicle applications. This patent does not include any discussion on lip separation problem in forward flight regime.

Bright, 2,968,453 (1961): Bright [23] presented an early form of the two well known and more recent vehicle concepts from Yoeli [24] (Xhawk) and Piasecki [25] (Piasecki Air Jeep). Two ducted fans are embedded into a relatively flat fuselage with two fixed wings extending from the sides of the fuselage. An extensive adjustable shutter based exit flow control system was used to control the side force, yaw, pitch and roll motions of the vehicle. Inlet flow to the ducted fan units were not treated using louvers, vanes or shutters of any kind. Leading side lip separation problem is not mentioned.

Fletcher, 2,988,301 (1961): A V/STOL aircraft concept using a counter rotating ducted fan embedded in a flat airfoil shaped fuselage was presented by Fletcher [26] in an effort to transist a V/STOL aircraft to propel itself in high speed flight. Forward flight related propulsive force was obtained from a conventional propeller mounted on the aft section of the vehicle. This vehicle has a provision to close the inlet surface of the fan rotor

system completely in forward flight only relying on the lift force generated by the airfoil shaped fuselage and the propulsive force of the aft propeller. Inlet lip separation problem inherent to most ducted fan based systems of this type was never mentioned in this reference.

Piasecki, 3,184,183 (1965): This patent[25] explains Frank Piasecki's well publicized "Air Jeep" concept shown in Figure 1.6 that uses two counter rotating lifting rotors in a tandem ducted fan arrangement. This approach was unique because of a novel control linkage for its ducted vertical lift rotors for adjusting cyclic pitch and collective pitch of the rotating blades. The propulsive force in Piasecki's approach [25] was obtained by cyclic and collective control of the rotor blades operating in a ducted fan arrangement. The rotor performance variation affected the local flow features near the leading side lip section of the duct. A significant component in this patent was the use of a movable spoiler in the inner part of the leading side lip of the duct. A movable spoiler that had a serrated edge is used to control local flow characteristics over the lip radius in an effort to reduce the drag (aerodynamic loss) generated over this area, especially in horizontal flight. This is one of the first known attempts to correct the inlet lip separation problem using a movable spoiler located over an arc length of the inlet lip. However, the specific corrective action taken for the lip separation problem is based on adjustable inlet boundary layer tripping.

Boyd, 3,159,224 (1970): This invention from Boyd [27] focused on a circular aircraft using an outer circumferential fan type ducted rotor mounted on air bearings. The ducted rotor was driven by outboard gas generators. This system used adjustable radial stator blades above the rotor. The stator blades were differentially adjustable in the forward and rearward quadrants to control the attitude of the aircraft with respect to its pitch axis. The stator blades in the left and right side quadrants could control the attitude of the aircraft with respect to its roll axis. The heading of the aircraft was controlled by means of a set of radial stator blades at the exit of the rotor. This approach only deals with the attitude control of a circular V/STOL vehicle and there is no treatment in this document in regard to possible inlet lip separation problem.

Wen 4,049,218 (1977): Wen *et al.*[28] described a VTOL aircraft using a centrifugal impeller generating a fan exit jet that can attain high exit jet velocities for effective vertical take off. His concept is shown in Figure 1.7. The centrifugal impeller output is passed through a diffuser section and

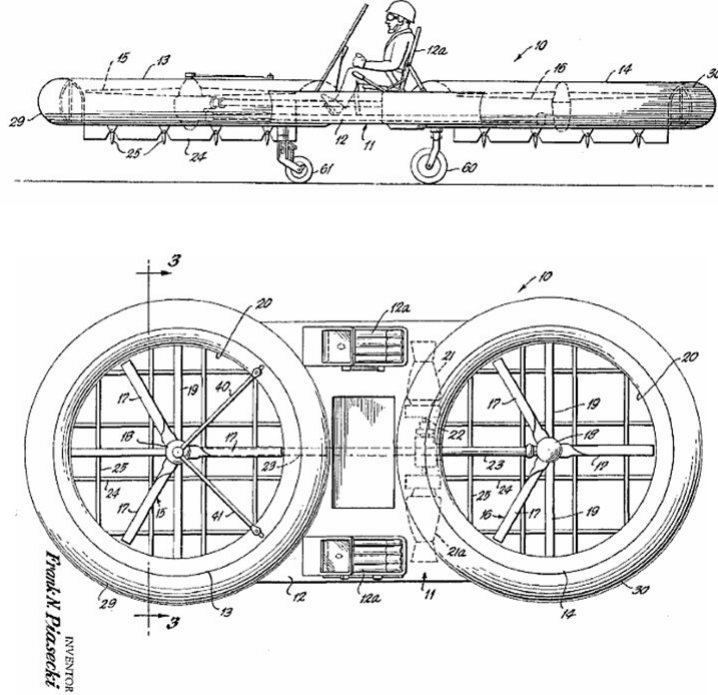


Figure 1.6: Piasecki air jeep [25]

deflected down to lift the aircraft. The impeller may be retracted down along its axis of rotation during transition to horizontal flight. The impeller exit is directed towards an exit nozzle at the aft section of the aircraft for the horizontal thrust needed for transition and forward flight. Although this is an interesting concept utilizing a centrifugal fan, its inlet flow characteristics and the influence of inlet flow distortion on the fan performance are not discussed in this patent document [28].

Moller, 4,795,111 (1989): One of the earliest patents is a flying robotic platform using a conventional ducted fan and a set of two mutually perpendicular vane systems from Moller [4]. The patent focuses on flexible variable camber flaps and exit flow control features which are illustrated in Figure 1.8 with no mention of inlet lip separation problem for this type of vehicle. Radio control of flexible control surfaces and unique arrangements of spoilers and flaps are described.

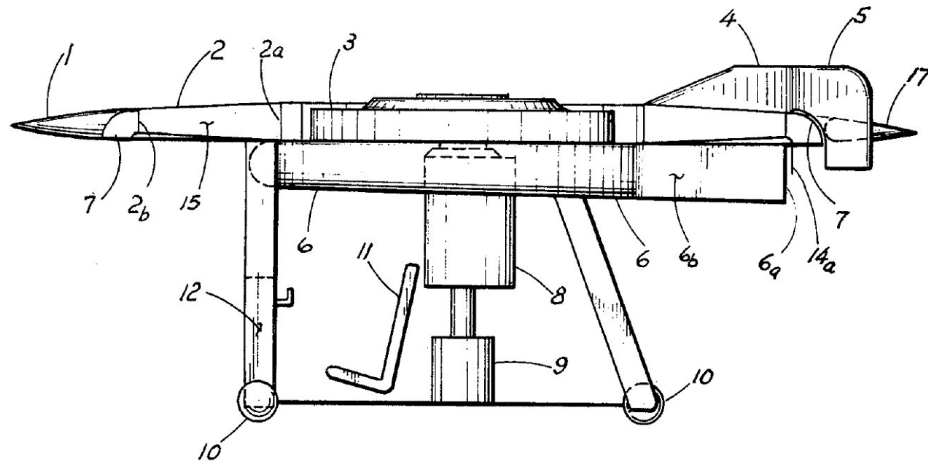


Figure 1.7: Side view and a partial section of a VTOL design by Wen et al.[28]

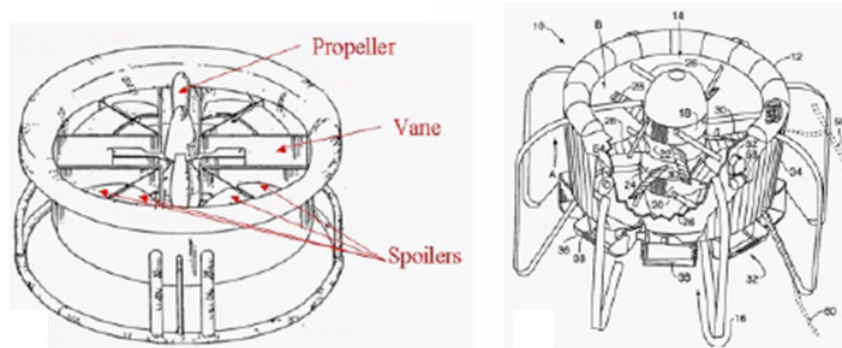


Figure 1.8: Control vanes, spoilers and thrust reverser designs of Moller [4]

Cycon et al.5,152,478 (1992): Sikorsky Cypher [29] shown in Figure 1.9 was an uninhabited aerial vehicle that included a toroidal fuselage and two co-axial counter-rotating rotors in a ducted fan arrangement. The two rotors provided both the vertical and horizontal thrust needed in hover and forward flight. A vertical take off required a completely horizontal operation for obtaining a vertical down wash of the rotors to obtain the necessary

lift for the aircraft. Transition to forward flight was achieved by tilting the fuselage in a “*Nose-down*” mode to generate a horizontal thrust component. In the forward flight mode, the rotor inlet flow was usually altered such that the leading side lip had significant flow separation and the trailing side of the duct had incoming flow impinging on the inner side of the shroud creating a drag penalty. The inlet nose separation, impingement on the aft part of the shroud and the interaction of this inlet flow distortion with the rotors resulted in significant pitch-up moment generation on this vehicle. Cypher is one of the few VTOL vehicles that used cyclic pitch of the rotors in encountering the nose-up pitch pitching moment generation. Although this control feature unique to Cypher reduced the excessive pitching moment, it required considerable amount of power and did not eliminate the drag generation on the trailing side of the shroud.

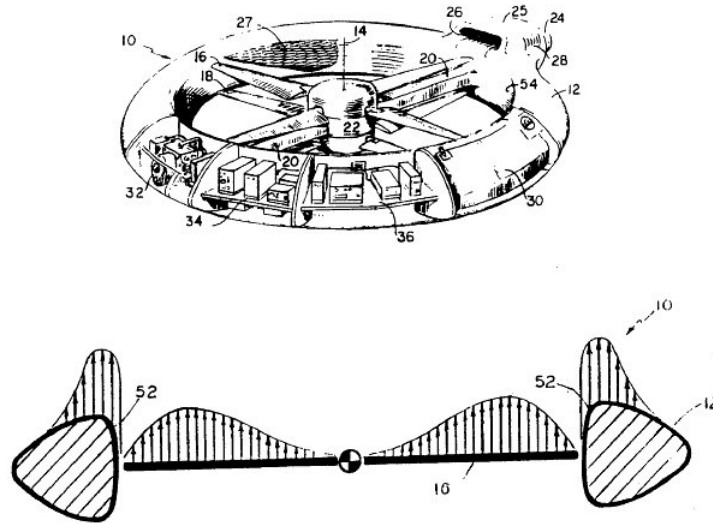


Figure 1.9: Sikorsky Cypher I with two co-axial counter-rotating rotors in a ducted fan arrangement [29]

Moffit et al.5,150,857 (1992): Another solution in reducing the pitching moment was the use of an optimized toroidal fuselage airfoil profile, Moffit et al.[30] The cross sectional geometry of the toroidal airfoil was optimized such that the increasing pitching up moment with increased forward flight velocity was measurably reduced. The pitching up moment reduction

was very effective from 20 knots vehicle speed up to 70 knots, which was the maximum flight velocity tested in a wind tunnel. The lift of the shroud was also effectively increased via this toroidal fuselage airfoil optimization. While incorporation of an optimized toroidal airfoil was a viable option, to counteract nose-up pitching moments, there was a manufacturing penalty associated with the new profile and an adverse effect on higher speed flight characteristics.

Flemming et al.5,419,513 (1995): Adding a highly cambered fixed wing to a toroidal fuselage was a significant method of dealing with excessive pitch-up moment generation encountered in forward flight of Cypher. Flemming et al.[31] used a high-lift high-camber airfoil with a center of lift located significantly aft of the quarter chord line of the airfoil. The symmetrically mounted fixed wings had centers of lift located aftwardly of the fuselage axis of the toroidal fuselage in forward flight mode such that the fixed wings generate a nose-down pitching moment to counteract the nose-up pitching moment originating from the separated air flow over the leading side lip of the duct. The fixed wings were mounted in a fixed arrangement at a predetermined angle of incidence although a variable incidence system for the fixed wing is possible.

Swinson et al.5,890,441 (1999): An autonomously controlled, gyroscopically stabilized, horizontal and vertical take off and landing (HOVTOL) vehicle using vertical lift devices was presented by Swinson et al.[32]. Although this vehicle had similarities to most of the systems reviewed in this section, the specific patent focused on the autonomous controllability of the vehicle rather than the aerodynamic features and inlet lip separation problem.

Cycon et al.6,170,778 (January 2001): A new method of reducing nose-up pitching moment during forward flight on a ducted uninhabited aerial vehicle was presented by Cycon et al.[33] The vehicle shown in Figure 1.10 consisted of a doughnut shaped fuselage that had a counter rotating ducted fan with fixed wings attached to it for improved forward flight characteristics. The system also had a shrouded pusher propeller for horizontal thrust in forward flight. Cycon et al.[33] used the method of adding high lift cambered airfoils to the sides of the toroidal fuselage of Cypher to counteract the nose-up moments generated in forward flight. The specific fixed wings also had flaperons for the precise adjustments of lift forces needed at different horizontal flight regimes. This system also had directional turning

vanes at the aft section of the pusher propeller to deflect propeller thrust downward, creating additional lift to counteract nose up moments in high speed forward flight. They also noted that locating the pusher prop assembly aft of the duct reduced drag on the aircraft. The pusher prop has been found to draw turbulent air over the duct that would otherwise flow into the duct. Cycon [33] also suggested an excellent way of concealing the rotor system in high speed flight. Conventional systems used relatively heavy and complex covers to block the air entrance to the ducted fan in high speed forward flight. Operating the counter rotating rotors at zero pitch resulted in a virtual cover system impeding the airflow into the duct. By blocking the flow and forcing it to flow over and under the aircraft, drag was effectively reduced without the weight and complexity of rigid covers.

Cycon et al.6,270,038 (August 2001): In addition to the flaperons in the fixed wings and the directional turning vanes in the propeller shroud exit, this invention [34] reported one or more deflectors mounted to the bottom of the fuselage for further drag reduction. The deflectors effectively controlled airflow into the duct from the bottom of the fuselage during forward flight. These deflectors were passive and required no actuation. They opened and closed automatically based on the airflow through and over the duct. The combination of zero pitch counter rotating rotors and passive flow deflectors on the bottom of the duct reduced the drag component on the aircraft between the open rotor and completely covered duct by about 80 %.

Moller, 6,450,445 (2002): A remotely controlled flying platform or a robotic platform was previously presented by Moller [4]. This concept more recently presented by Moller [35] used a counter rotating set of axial rotors in a ducted fan arrangement. Although an extensive set of fan exit flow control surfaces were used in this system, the inlet lip separation problem was not mentioned. The specific exit flow control surfaces are named “*multiple adjustable air deflector assemblies*” controlled by two servo motors. The invention focuses on the actuation of the individual air deflectors via servo mechanisms.

Yoeli, 6,464,166 (2002): This approach introduced by Yoeli [24] uses a plurality of parallel spaced vanes located in front of and behind the ducted fan rotor of a VTOL vehicle illustrated in Figure 1.11. The vanes are selectively pivotal to produce a desired horizontal force component to the lift

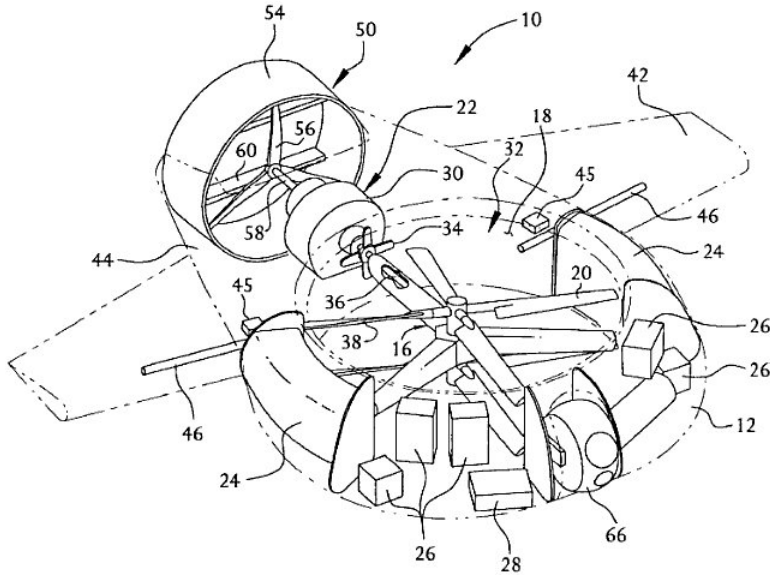


Figure 1.10: Sikorsky Cypher II with pusher propellers [34]

force applied to the vehicle. Many vane arrangements are presented for producing side force, roll, pitch and yaw movements of the vehicle. Symmetrical airfoil sections spaced at one chord length from each other are used. Each vane is split into two halves, each half of all the vanes are being separately pivotal from the other half. This method does not deal with any aspects of upstream lip separation that will occur especially during horizontal flight of this VTOL vehicle.

Wagner 6,886,776 (2005): A VTOL personal aircraft (PAC) comprising of a fixed wing a fuselage and multiple of independently powered thrusters was explained by Wagner [36]. The thrusters preferably integrated into the wing generated a flight system with a lift to drag ratio equal or greater than two. At least one thruster on each side of the fuselage preferably comprised a “levitator” to create additional lift from the airfoil like air inlet. Although multiple of ducted fan units were utilized on both sides of the fuselage, the inlet lip separation problem was not mentioned in the manuscript.

Yoeli, 6,883,748 (2005): This invention [37] deals with the use of two ducted fans, four ducted fans and multiple free propellers on VTOL vehicle types already discussed by Yoeli in his previous patents. In addition to many military configurations possible with this vehicle, a hovercraft version using a flexible skirt extending below the fuselage is discussed.

Yoeli, 0,034,739 (2007): A ducted fan based VTOL vehicle including a fuselage having a longitudinal axis and a transverse axis, two counter rotating ducted fan lift producing propellers are described by Yoeli [38]. Many variations are described enabling the vehicle to be used not only as a VTOL vehicle, but also as a multi function utility vehicle. An unmanned version of the same vehicle is also described. Although an extensive use of inlet louvers and exit control surfaces are in place, there is no mention of an inlet lip separation control system near the leading side of the fans. The specific approach uses means for enabling the external flow penetrating the walls of the forward ducted fan for minimizing the momentum drag of the vehicle.

Yoeli, 7,275,712 (2007): This patent [39] described an enhancement of his 2002 concept [24] of parallel spaced vanes located in front of and behind the ducted fan rotor of a VTOL vehicle. Additional vane arrangements were presented for producing side force, roll, pitch and yaw movements of the vehicle. The left and right sides of the circular area at the rotor inlet and exit had parallel spaced vanes that were not in the direction of horizontal flight. The angle between the vanes and the flight direction was about 45 degrees for this specific patent. This patent did not have any description of inlet lip separation problem.

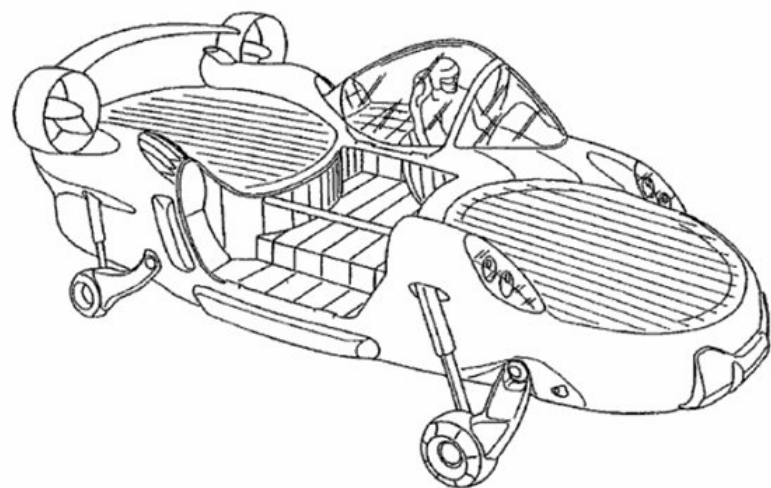
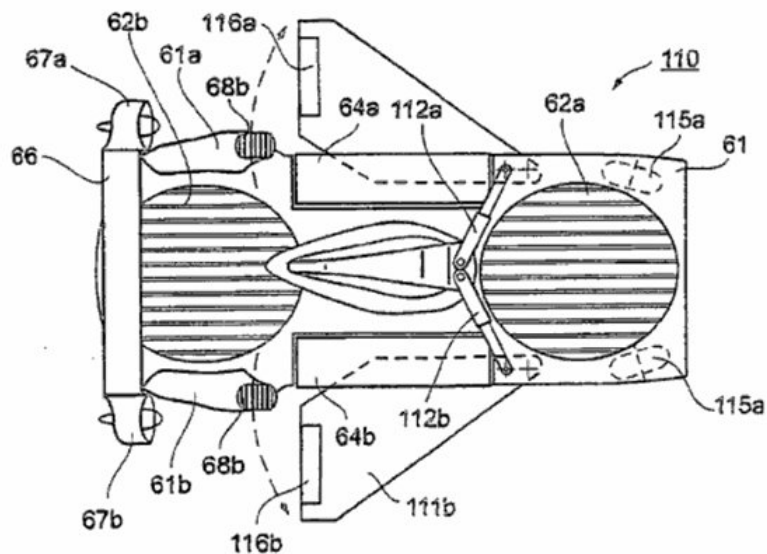


Figure 1.11: A ducted fan based VTOL vehicle including a fuselage having a longitudinal axis and a transverse axis, two counter rotating ducted fan lift producing propellers [24, 37–39]

Chapter 2

Double Ducted Fan (DDF) as a Novel Concept

A novel ducted fan concept as a significant improvement over a standard ducted fan is explained in Figure 2.1. The poor forward flight characteristics of the reference duct as shown in Figure 2.1a are effectively improved with the “*Double Ducted Fan*” concept as presented in Figure 2.1b. A typical deficiency of a standard ducted fan is mainly related to the forward lip separation increasingly occurring when the forward flight velocity is gradually increased as shown in the streamline patterns of Figure 2.1a.

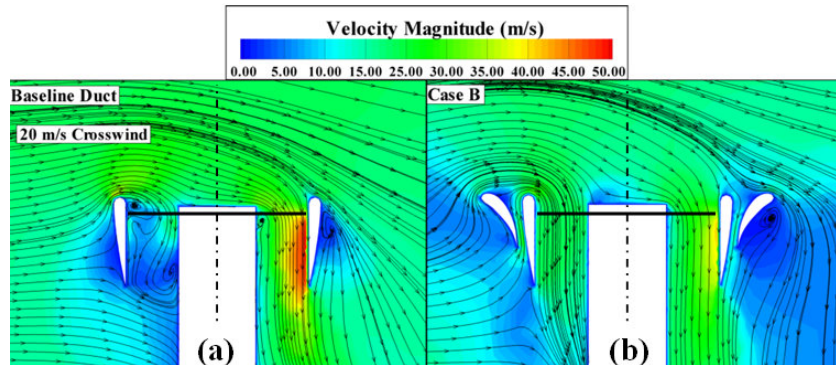


Figure 2.1: Separated flow near the forward lip section of a standard ducted fan (left) and the flow improvements from the novel concept Double Ducted Fan (DDF) at 9000 rpm, colored by the magnitude of velocity

The inlet flow near the leading side of the standard duct is highly separated, low-momentum and turbulent. The apparent flow imbalance between

the leading side and trailing side of the standard ducted fan as shown in Figure 2.1a is also called an “*inlet-flow-distortion*”. Flow simulations in Figure 2.1a show that the rotor barely breathes at the inlet section of the leading side although the trailing side passes a significant amount of flow. This flow imbalance amplified during the rotor “*energy adding process*” is one of the reasons of significant nose-up pitching moment generation. Figure 2.1b also presents the Double Ducted Fan (DDF) flow simulations indicating the effective inlet flow distortion reduction due to the unique aerodynamic properties of the (DDF) system. The upstream lip separation near the leading side is almost eliminated resulting in a more balanced rotor exit flow field between the leading side and the trailing side. More detailed descriptions of the local flow field improvements resulting from the novel Double Ducted Fan (DDF) concept are discussed in the final part of this document. Although there may be many other potentially beneficial variations of the Double Ducted Fan concept, only the specific (DDF) form defined in Figure 2.1b will be explained in detail in the preceding sections.

2.1 Geometric Definition of DDF

The DDF concept uses a second duct using a lip airfoil shape that has a much shorter axial chord length than that of the standard duct. The key parameter in obtaining an effective DDF arrangement is the size of the lip diameter D_L of the standard ducted fan. The second duct airfoil that is relatively cambered has a leading edge diameter set to 0.66 D_L as explained in Figure 2.2b. The angular orientation and axial position of the second duct airfoil is extremely important in achieving a good level of flow improvement near the leading side of the rotor. The leading edge circle of the second duct airfoil is slightly shifted up in the vertical direction for proper inlet lip separation control. The vertical distance between the duct inlet plane touching the standard duct and the plane touching the second duct is about $0.33D_L$ as shown in Figure 2.2b. The horizontal distance between the centers of the leading edge circles of the standard duct and outer duct is about $4D_L$. The axial chord of the second duct airfoil is about $5D_L$. The separation distance between the standard duct and second duct is controlled by the recommended throat width of $0.8D_L$ as shown in Figure 2.2b.

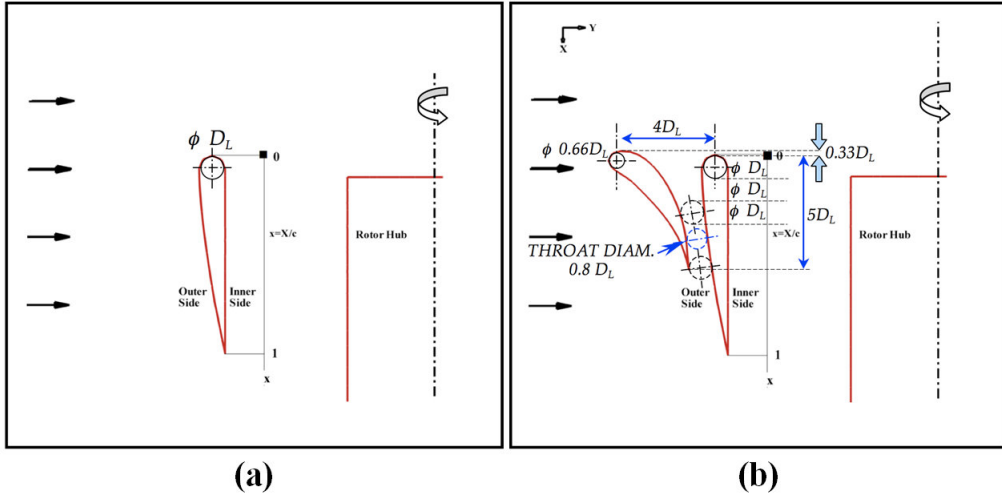


Figure 2.2: (a)Reference duct airfoil definition in a standard ducted fan arrangement, (b)Double Ducted Fan (DDF) geometry as a novel concept

2.2 Converging-Diverging Channel in the Duct

The second duct and the standard duct forms a converging-diverging channel starting from the trailing edge of the second (outer) duct that is located at about $X=5D_L$. The axial position of the throat section is about $0.45c$ where c is the axial chord of the inner duct as shown in Figure 2.2b. The duct width at the entrance of the converging-diverging duct is D_L . The entrance to the converging-diverging channel is at the trailing edge point of the second duct. There is a (vertically up) net flow in the converging-diverging duct of the DDF. This flow is due to increasing dynamic pressure at the entrance of the converging-diverging duct at $X=5D_L$ when the forward flight velocity is increased. The diverging part of the channel flow between the standard and outer duct is extremely important in this novel concept, since this decelerating flow is instrumental in adjusting the wall static pressure gradient just before the lip section of the leading edge of the standard duct. The self-adjusting dynamic pressure of the inlet flow into the converging-diverging duct is directly proportional with the square of the forward flight velocity of the vehicle. The converging-diverging duct flow is in vertically up direction near the leading edge of the vehicle. The flow in the intermediate channel is vertically down when one moves away from the frontal section of the vehicle. This flow direction is caused by the relatively low stagnation

pressure at the inlet of the intermediate channel at circumferential positions away from the leading edge. This vertically down flow induced by the static pressure field of the inner duct exit flow is likely to generate measurable additional thrust force for the DDF based vehicle.

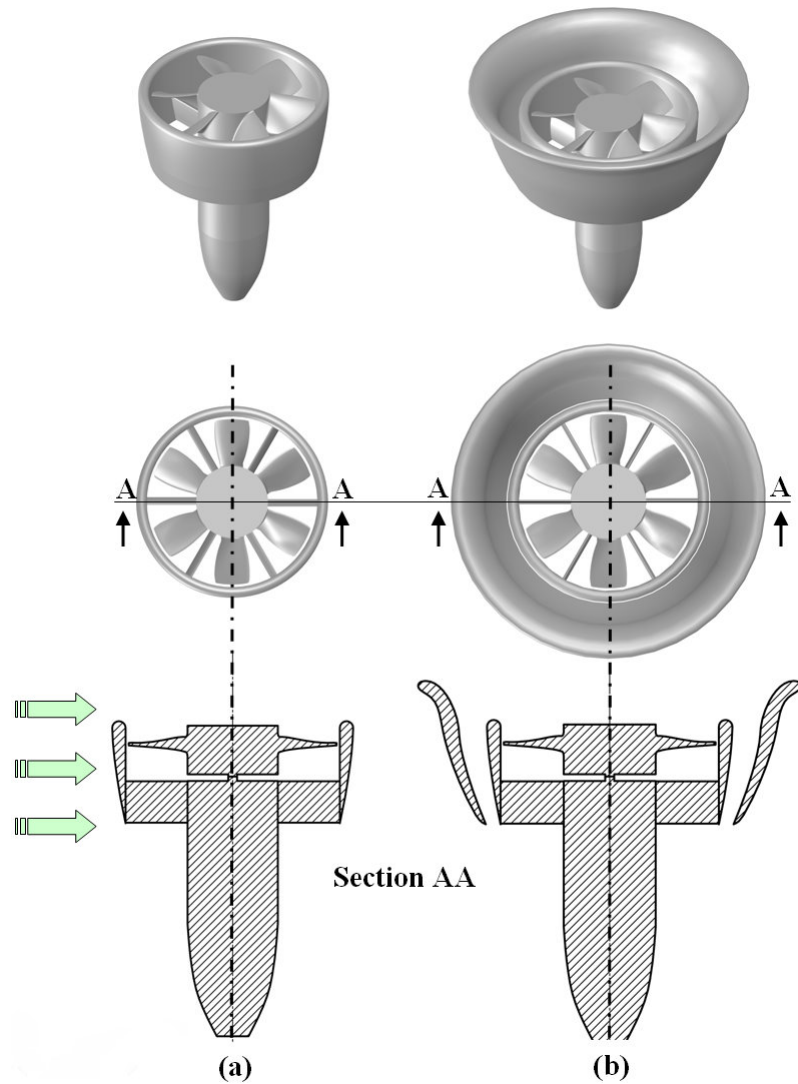


Figure 2.3: (a)Baseline ducted fan (Standard duct), (b)CASE-A tall double ducted dan (DDF)

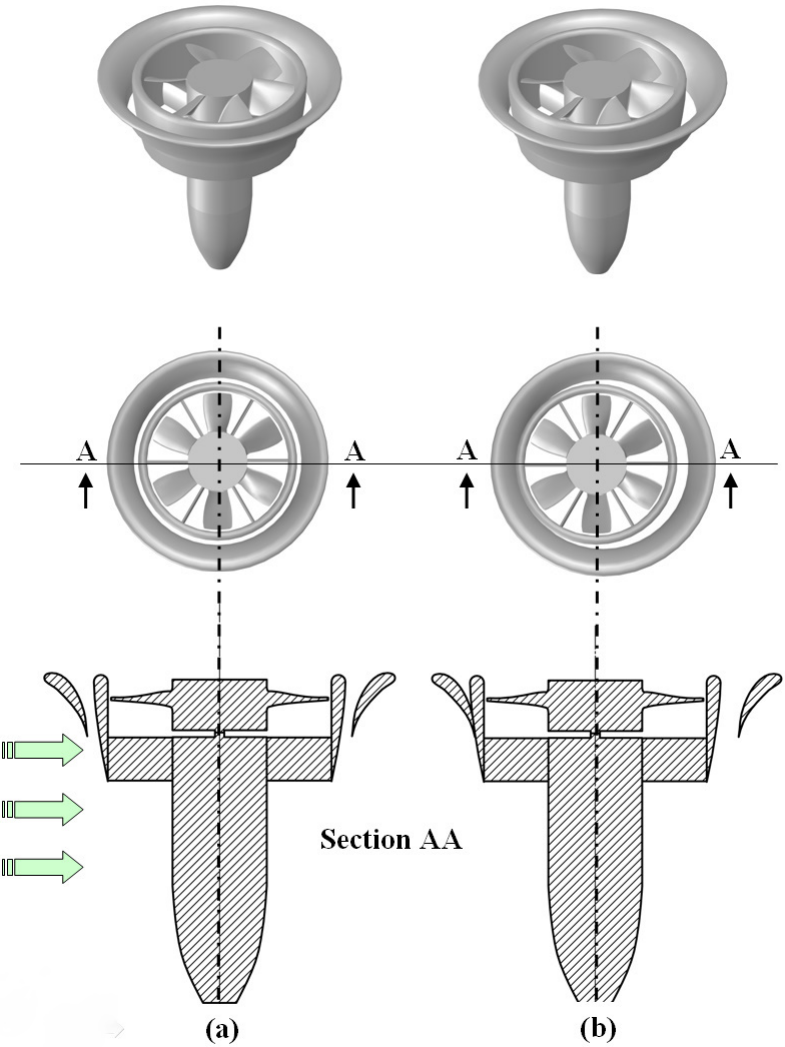


Figure 2.4: (a)CASE-B short double ducted fan (b)Eccentric double ducted fan

2.3 Various Possible Double Ducted Fan Geometries

The standard duct and three possible variations of the Double Ducted Fan (DDF) concept described in this study are presented in Figures 2.3 and 2.4. Three dimensional solid models of the four duct configurations, a hor-

izontal cross section and a vertical cross section are included in these figures.

CASE-A as shown in Figure 2.3b is termed as the tall DDF. The tall DDF is able to generate a significantly higher thrust in hover position than that of the standard duct containing an identical rotor. However, in forward flight, due to the extended axial chord of the outer duct, the nose-up pitching moment generation is also significant in this design. This design has a throat section located at the trailing edge of the duct airfoils. Since the axial chord of the outer duct is longer than that of the inner duct this design may have a drag penalty when compared to the standard ducted fan.

Figure 2.4a shows the most effective Double Ducted Fan (DDF) configuration CASE-B since it has the ability to generate a significant amount of thrust when compared to that of the standard ducted fan configuration. Another important characteristic of CASE-B is its ability to operate without enhancing the nose-up pitching moment of the vehicle in forward flight. This configuration was analyzed in great detail mainly because of its combined ability to enhance thrust and reduce nose-up pitching moment in forward flight without a significant drag increase.

An ECCENTRIC DOUBLE DUCTED FAN (DDF) concept is also shown in Figure 2.4b. This concept requires a movable outer duct in order to control the throat area in the intermediate duct of the vehicle for a highly optimized forward flight performance. Variable throat mechanism introduced in this concept provides a greater range of operation in a DDF type vehicle offering a more accurate lip flow control over a much wider forward flight velocity range. Figure 2.4b shows a highly blocked second duct that is proper for very low forward flight velocity. It is required that the throat area is enlarged by moving the outer duct as the forward flight velocity is increased. Although an almost optimal lip separation control can be achieved with an eccentric (DDF), its mechanical complexity and weight penalty is obvious. The outer duct airfoil definition of this concept is the same as CASE-B that is described in detail in Figure 2.2b.

Chapter 3

Method of Analysis used in (DDF) Concept Development

A three dimensional simulation of the mean flow field around the ducted fan was performed using a custom developed radial equilibrium based rotor disk model implemented into the commercial code Ansys/Fluent. The specific computational system solves the Reynolds Averaged Navier-Stokes (RANS) equations using a finite volume method.

3.1 Radial Equilibrium Based Analysis of Ducted Fan in Hover and Forward Flight

3.1.1 Computational Model Description

A simulation of the mean flow field around the ducted fan was performed by using a commercial code Ansys-Fluent [40]. The specific computational system solves the 3D Reynolds-Averaged Navier-Stokes equations using a finite volume method. The transport equations describing the flow field are solved in the domain that is discretized by using an unstructured computational mesh. For the analysis of the flow field around ducted fan rotors, there are many computational modeling options in general purpose fluid dynamics solvers. The most complex and time consuming computational model is the modeling of unsteady/viscous/turbulent flow in and around the fan rotor by using an exact 3D model of rotor geometry using a sliding mesh technique.

This type of solution is usually lengthy and requires significant computer resources especially in the forward flight mode when an axisymmetric flow assumption is not applicable. The current RANS computations use a simplified rotor model termed as “*Actuator disk model*” for the generation of the general inviscid flow features of the fan rotor. A $k - \epsilon$ turbulence model was invoked for the current computations, in areas other than the actuator disk. Figure 3.1 shows a flowchart of the method used.

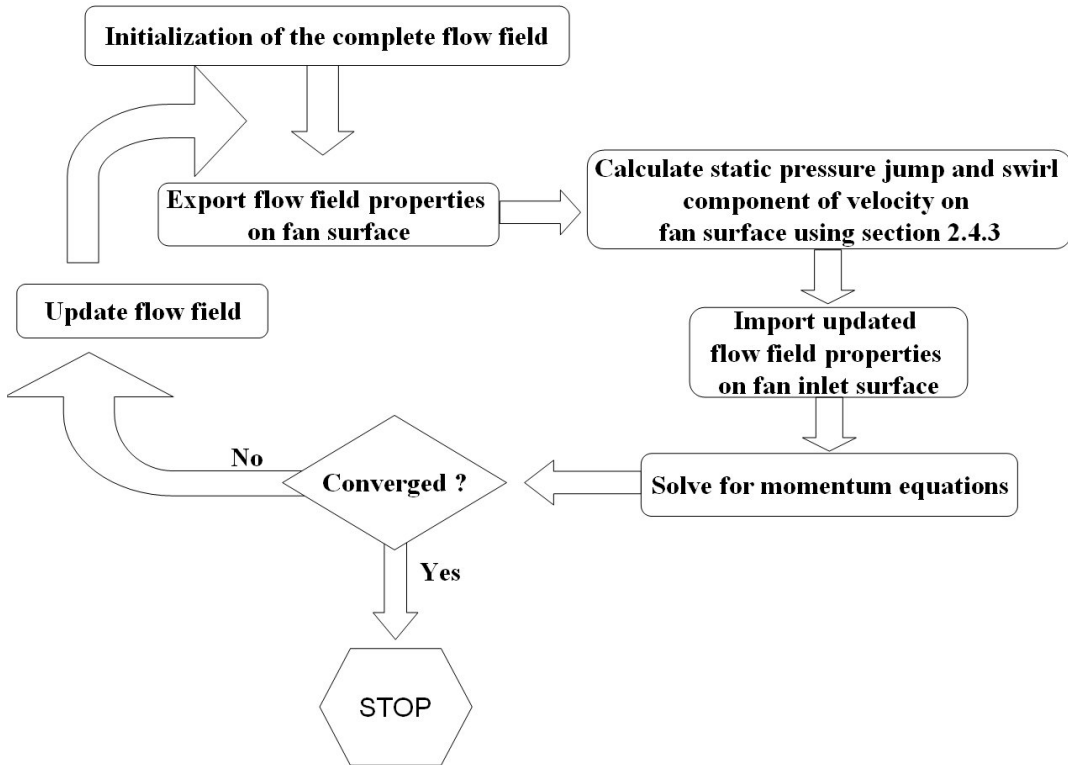


Figure 3.1: Flowchart of the 3D RANS based computational method including the actuator disk.

3.1.2 Boundary Conditions

Hover

Figure 3.2 shows the specific boundary conditions and computational domain size implemented in the solver for hover condition. The duct and

tailcone surfaces are considered as solid walls with no-slip condition. On the side surfaces, a symmetry condition is assumed. For the hover condition, a pressure inlet boundary is assumed on the top surface. Atmospheric static pressure is prescribed on the top surface. Pressure inlet boundary is treated as loss-free transition from stagnation to inlet conditions. The solver calculates the static pressure and velocity at the inlet. Mass flux through boundary varies depending on interior solution and specified flow direction. Pressure outlet boundary condition is assumed on the bottom surface for hovering condition. Pressure outlet boundary interpreted as atmospheric static pressure of environment into which the flow exhausts. An additional “Fan” type condition was used for the implementation of the specific actuator disk model described in section 3.1.3.

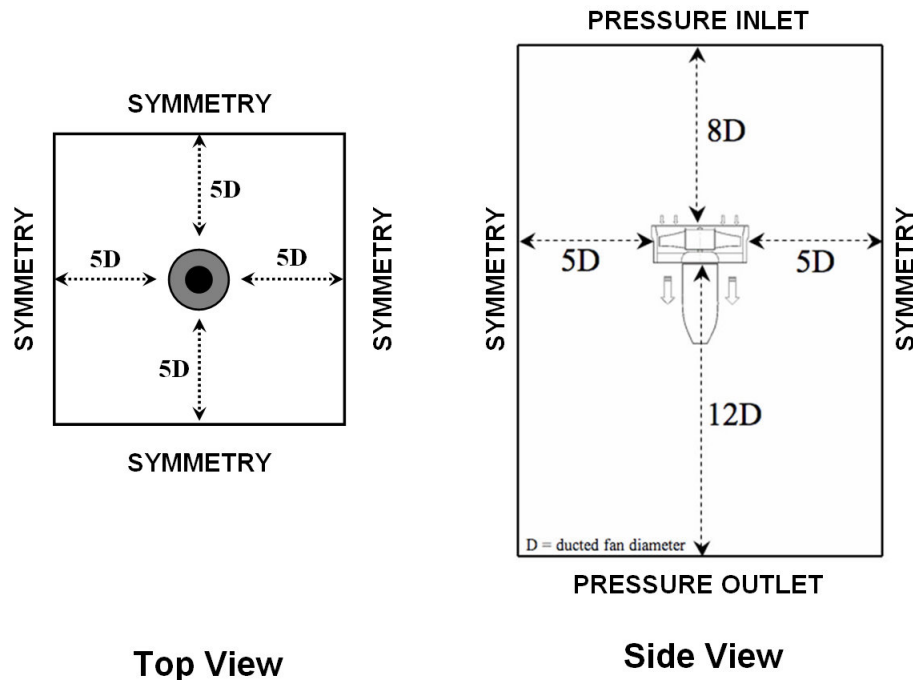


Figure 3.2: Boundary conditions for hover

Forward Flight

Figure 3.3 shows the specific boundary conditions implemented in the solver for forward flight. Like hover condition, the duct and tailcone surfaces are considered as solid walls with no-slip condition. Velocity inlet boundary condition is assigned on the windward side of the computational domain. Using this boundary condition velocity and turbulent intensity at the windward side is prescribed. For the leeward side of the domain an outflow condition is assigned. For the top, bottom and remaining side surfaces symmetry boundary condition is assigned. Like the hover condition, “*Fan*” type condition was set using an “*actuator disc model*” replacing the ducted fan rotor. Details of the actuator disk model is explained in section 3.1.3.

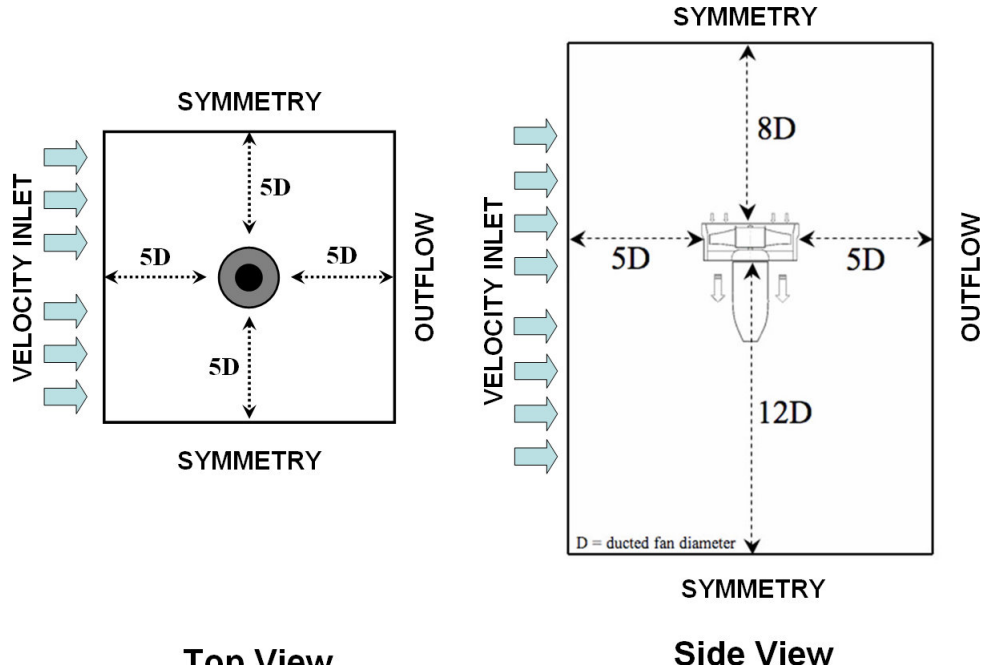


Figure 3.3: Boundary conditions for forward flight

3.1.3 Actuator Disk Model

The complex 3D rotor flow field in the rotating frame of reference is replaced by a simplified “*actuator disc model*” originating from the simultaneous use of the radial equilibrium equation, energy equation and the conservation of angular momentum principle across the fan rotor. The radial equilibrium equation is the force balance in the radial direction at a given axial position, balancing the pressure forces in radial direction with the centrifugal force. The viscous effects are ignored in this simplified and easy to implement “*actuator disc model*”.

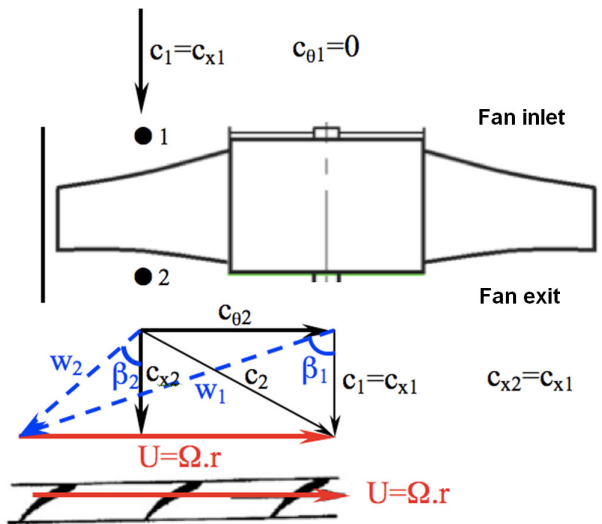


Figure 3.4: Velocity triangles at the inlet and exit of the ducted fan rotor

In this approach, a pressure change term is computed at each radial position of the rotor from hub to tip. The magnitude of the static pressure jump term across the rotor is closely related to the amount of stagnation enthalpy change from the rotor inlet to exit. The stagnation enthalpy increase from the rotor inlet to exit is the same as the rate of energy provided to the fluid by the rotor per unit mass flow rate of the duct flow. The conservation of angular momentum principle and energy equation suggests that the magnitude of this jump is mainly controlled by the tangential (swirl) component $c_{\theta 2}$ of the flow velocity in the absolute frame of reference at the exit of the rotor and rotor angular velocity.

Figure 3.4 presents the velocity triangles of the ducted fan rotor at inlet (1) and exit (2). β_1 and β_2 are the blade inlet and exit angles measured from the axial direction. Since the tip Mach number (0.28) of the rotor is not in the compressible flow range, it is reasonable to assume that the internal energy at the rotor inlet e_1 and exit e_2 is the same, $e_1=e_2$. In a ducted fan rotor, it is realistic to assume that the “*axial component*” of the absolute velocity vector is also conserved from inlet to exit $c_{x2}=c_{x1}$. The flow is assumed to be axial at rotor inlet where $c_1=c_{x1}$ and $c_{\theta1} = 0$ under design conditions. The relative velocity vector at the exit of the rotor w_2 is smaller than the relative velocity w_1 at the rotor inlet. While the relative flow w_2 is diffusing in the relative frame of reference, the absolute flow velocity vector c_2 is accelerated at the rotor exit, because of added energy to the flow by the rotor.

Equation 3.1 represents the change of stagnation enthalpy in the ducted fan rotor system. The right hand side of this equation is the rate of work per unit mass flow rate of air passing from the rotor. The right hand side is also the same as the product of the rotor torque and angular speed of the fan rotor.

$$h_{O2} - h_{O1} = U(c_{\theta2} - c_{\theta1}) \text{ where } U = \Omega r \text{ and } c_{\theta1} = 0 \quad (3.1)$$

$$(h_2 + c_2^2/2) - (h_1 + c_1^2/2) = U c_{\theta2} \quad (3.2)$$

$$\left(e_2 + \frac{p_2}{\rho_2} + c_2^2/2 \right) - \left(e_1 + \frac{p_1}{\rho_1} + c_1^2/2 \right) = U c_{\theta2} \quad (3.3)$$

Equation 3.1 is a simplified form of the energy equation from rotor inlet to exit of a ducted fan unit. When $e_1=e_2$ is substituted into equation 3.3 because of incompressibility condition, the “*Euler equation*” or “*pump equation*” results in as equation 3.4. Using equations 3.4 and 3.5, an equation for the calculation of static pressure jump between the rotor inlet and exit can be obtained.

The determination of $c_{\theta2}$ is performed by using the velocity triangles in Figure 3.4. Since the blade inlet/exit angle distribution for 1 and 2 in radial direction is known from the existing rotor geometrical properties, shown in Table 4.1. w_2 can be calculated from the assumption that $c_{x2}=c_{x1}=c_1$. The absolute rotor exit velocity c_2 is determined by adding $U = \Omega r$ to w_2 in a

vectorial sense.

$$\frac{1}{\rho} (P_{O2} - P_{O1}) = U c_{\theta 2} \quad (3.4)$$

$$\left(p_2 + \rho \frac{c_2^2}{2} \right) - \left(p_1 + \rho \frac{c_1^2}{2} \right) = \rho U c_{\theta 2} \quad (3.5)$$

$$\Delta p = p_2 - p_1 = \rho \left[U c_{\theta 2} - \frac{1}{2} (c_2^2 - c_1^2) \right] \quad (3.6)$$

Equation 3.6 allows enforcing a prescribed pressure jump Δp in function of density, radial position, rotor angular speed Ω , rotor exit swirl velocity $c_{\theta 2}$, c_1 and c_2 . The rate of energy (per unit mass flow rate) added to the flow by the rotor is specified by the product $U c_{\theta 2}$ as shown in equations 3.4 and 3.5. Equation 3.6 could be evaluated at each radial position between the rotor hub and tip resulting in the radial distribution of the static pressure jump required by the general purpose viscous flow solver for a “*Fan*” type boundary condition. Δp can be effectively specified in a user defined function “*UDF*” in the solver (See Appendix ?? for details on UDF). The “*Fan*” type boundary condition is an effective and time efficient method of implementing a rotor flow field via an “*actuator disk model*” in a 3D viscous flow computation.

Details of the computational method can be found in [41].

Chapter 4

DDF Concept Validation

A three dimensional simulation of the mean flow field around the ducted fan was performed using a custom developed actuator disk model based on radial equilibrium theory implemented into the commercial code Ansys-Fluent. The specific computational system solves the Reynolds Averaged Navier-Stokes (RANS) equations using a finite volume method. Details of the computational method can be found in section 3.

4.1 Reference Ducted Fan Characteristics

Figure 4.1 shows the five bladed reference ducted fan that is used in the present DDF development effort. The relatively poor forward flight characteristics of the reference ducted fan shown in Figure 4.1 are significantly improved via the new double ducted fan (DDF) concept that is explained in the next few paragraphs. The geometric specifications of the reference ducted fan unit that is designed for small scale uninhabited aircraft are presented in table 4.1. This unit is manufactured from carbon composite material and has six vanes at the exit of the fan in order to remove some of the swirl existing at the exit of the rotor. A tail cone is used to cover the motor surface and hide the electrical wiring. All computational 3D flow simulations of the reference duct including the rotor flow field are performed at 9000 rpm using the geometry defined in Figure 4.1.

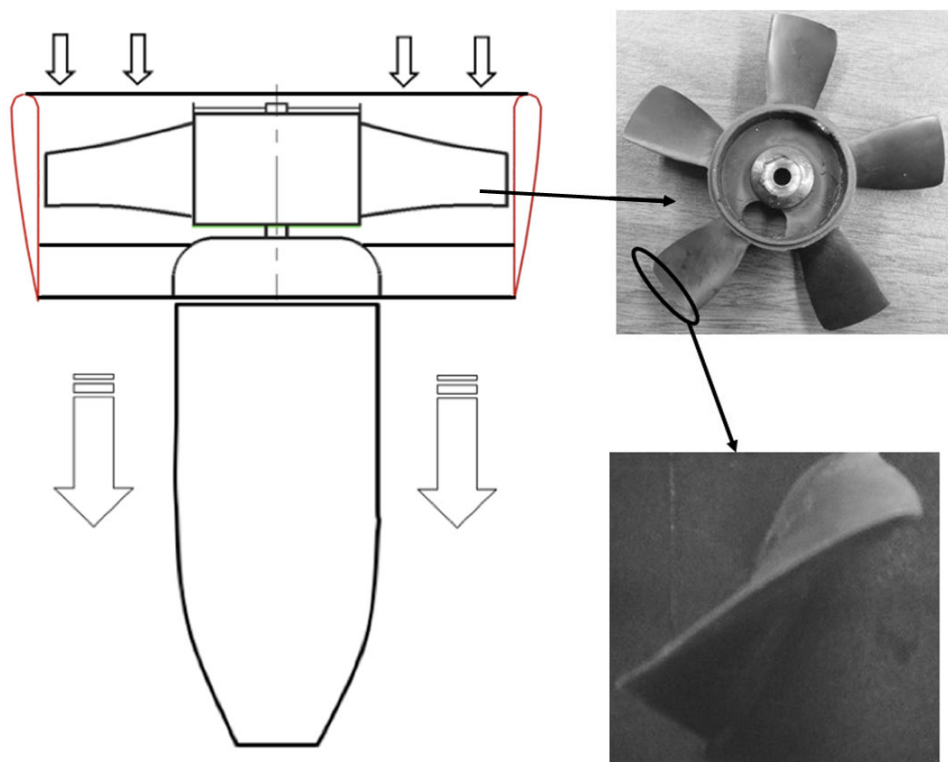


Figure 4.1: Reference ducted fan and fan rotor used for DDF development effort

Rotor hub diameter	52 mm
Rotor tip diameter	120 mm
Blade height h	34 mm
Tip clearance t/h	5.8 %
Max blade thickness at rotor tip	1.5 mm
Tailcone diameter	52 mm
Tailcone length	105 mm
Rotor blade section properties	
	Hub Mid Span Tip
Blade inlet angle β_1	60° 40° 30°
Blade exit angle β_2	30° 45° 60°
Blade chord	32 mm 30 mm 28 mm

Table 4.1: Geometric specifications of five inch ducted fan

4.2 Air Breathing Character of DDF in Forward Flight

Table 4.2 presents the computed fan rotor mass flow rate for all ducted fan types studied in this paper for both hover and forward flight conditions. In addition to hover conditions, the results are also presented for 10 m/s and 20 m/s forward flight velocities at 9000 rpm rotor speed that is constant for all computations.

	Fan Mass Flow Rate (kg/s)	Thrust (N)	Pitching Moment (N.m)	Flight Condition
Baseline Duct	0.30	3.04	0.00	No Crosswind (Hover)
Baseline Duct	0.29	3.47	0.17	10 m/s Crosswind
Baseline Duct	0.20	3.11	0.27	20 m/s Crosswind
MODIFIED DUCTS (DDF)				
CASE-A	0.31	5.02	0.00	No Crosswind (Hover)
CASE-A	0.31	4.93	0.37	10 m/s Crosswind
CASE-A	0.26	5.07	0.83	20 m/s Crosswind
CASE-B	0.30	3.02	0.00	No Crosswind (Hover)
CASE-B	0.30	3.72	0.16	10 m/s Crosswind
CASE-B	0.28	4.86	0.29	20 m/s Crosswind

Table 4.2: Computed rotor mass flow rate for all fan configurations during hover and forward flight

Constant rpm flow simulations provide a basis for comparisons of 3D mean flow, fan thrust, nose-up pitching moment, total pressure and static pressure fields. Although the rotor speed is constant for all computations, the amount of mechanical energy transferred to the air during its passage

through the rotor varies, because of highly varying inlet flow field into the ducted fan unit during hover, forward flight at 10 m/s and 20 m/s. Table 4.2 also provides the computational estimates of thrust, nose-up pitching moment for hover and forward flight conditions.

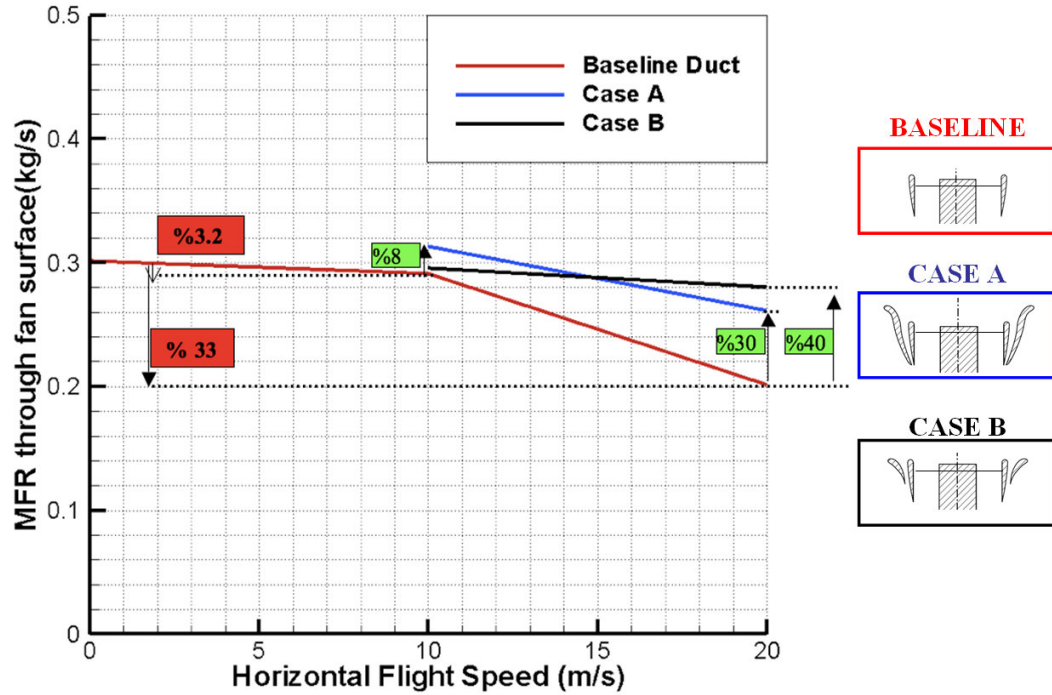


Figure 4.2: Rotor disk mass flow rate versus forward flight speed at 9000 rpm

Figure 4.2 shows that the baseline duct suffers from a high level of “*inlet flow distortion*” at 10 m/s and 20 m/s forward flight velocity. The overall mass flow rate passing from the ducted fan is reduced to 66 % of the hover mass flow rate as shown by the red line in Figure 4.2 (for 20 m/s forward flight). This significant limitation on the rotor mass flow rate is mainly the result of the large separated flow region occurring at just downstream of the lip section of the leading side of the duct as shown in Figure 2.1. While the leading side of the baseline duct passes a severely limited amount of air mass, the trailing side of the duct is able to breathe at a better rate than the leading side. It is apparent that the leading side of the baseline duct is partially blocked at high forward flight velocities. Figure 4.2 also shows a

significant drop in rotor mass flow rate when the forward flight velocity is increased from 10 m/s to 20 m/s.

Baseline duct mass flow rate, thrust and nose-up pitching moment: Table 4.2 contains nose-up pitching moment information for all flight regimes showing a measurable increase in the pitching moment when the baseline vehicle moves at 10 m/s and 20 m/s in comparison to hover conditions. The nose-up pitching moment is measured with respect to the center of gravity of the ducted fan unit for all cases. At 20 m/s forward flight condition, the predicted pitching moment is 1.6 times that of the pitching moment at 10 m/s flight velocity. The pitching moment generation on a typical ducted fan in forward flight is directly related to the extent of inlet lip separation, the impingement of the rotor inlet flow on the duct inner surface (aft shroud surface) on the trailing side of the duct, imbalance of the rotor exit field between the leading side (low momentum) and trailing side (high momentum), aerodynamic profiling of the duct outer surface especially near the leading side.

Predicted baseline ducted fan thrust values at 10 m/s and 20 m/s increase to 1.5 times and 1.7 times of the thrust of the baseline duct at hover conditions. This relative thrust improvement is due to the specific external shape of the baseline duct and modified rotor inlet conditions at elevated forward speed levels.

Mass flow rate, thrust and nose-up pitching moment characteristics of CASE-A : The air breathing character of the baseline duct can be significantly improved by implementing the tall double ducted fan (DDF) designated as CASE-A as shown in Figure 4.2. The mass flow rate of CASE-A is about 8 % more than that of the baseline duct operating at the forward speed of 10 m/s. The rotor mass flow rate improvement for CASE-A at 20 m/s is much higher than that of the baseline duct operating at 20 m/s. A 30 % improvement over the baseline duct is possible. This relative mass flow rate improvement is a direct result of reduced inlet lip separation near the leading side of the duct designs at forward flight.

The predicted thrust for the tall double ducted fan (DDF) CASE-A is markedly higher than that of the baseline duct. At 10 m/s horizontal flight velocity, the thrust of CASE-A is about 1.7 times that of the baseline duct. When the flight velocity is elevated to 20 m/s, CASE-B produces an augmented thrust value of 1.9 times that of the baseline duct. The reduction

of the inlet lip separation results in a direct improvement of the ducted fan exit flow near the leading side of the duct. The thrust improvements are due to both ducted fan exit flow improvements near the leading side of the unit, the external aerodynamic shape of the outer duct. The leading side of the DDF CASE-A rotor plane breathes air from the inlet at a much-improved rate than that of the trailing side. The tall (DDF) CASE-A also entrains a measurable amount of air into the outer duct from the inlet area of the unit especially near the trailing side. The flow in the outer duct is in opposite direction to the rotor flow near the leading side. However, the outer duct flow for the circumferential positions away from the leading side of the duct is in the same direction as the main rotor flow direction. Additional thrust augmentation is possible in the outer duct at positions away from the leading edge.

Although the tall (DDF) CASE-A is an excellent thrust producer at high forward flight velocities, it has the capability of augmenting the usually unwanted nose-up pitching moment mainly because of the external shape of the outer lip at elevated forward flight velocities. The pitching moment predicted at 10 m/s is about 2.2 times that of the baseline duct. At 20 m/s, the pitching moment produced by CASE-A is about 3.1 times that of the baseline duct value. The reason the short ducted fan CASE-B was designed and developed was the need to reduce the unwanted pitching up moment generation unique to CASE-A.

An effective DDF design CASE-B with highly reduced nose-up pitching moment: CASE-B as shown in Figure 4.2 is a shorter version of the double ducted fan design concept. CASE-B is designed to produce a significantly reduced nose-up pitching moment when compared to CASE-A. Another goal with CASE-B is to obtain similar thrust gains over the baseline duct. The short double ducted fan (DDF) CASE-B controls the lip separation as effectively as the tall (DDF) CASE-A without producing a high nose-up pitching moment. The airfoil geometry forming the outer duct has an axial chord length that is about half of the axial chord of the inner duct (also termed as standard fan or baseline fan). A detailed description of obtaining a short double ducted fan (DDF) CASE-B is given in Figure 2.2a. starting from a baseline duct. Figure 4.2 indicates that the mass flow rate improvement (black line) of CASE-B is very similar to CASE-A (blue line). The short (DDF) CASE-B's sensitivity to increasing forward flight velocity is much less when compared to tall (DDF) CASE-A. Implementation of a second duct as shown in Figure 2.2b enhances the lip separation controlled

flight zone further into higher forward flight velocities. The thrust values predicted for the short (DDF) are much higher than the standard duct predictions at 10 m/s and 20 m/s. There is a slight reduction in thrust when comparison is made against the tall (DDF) CASE-A. The most significant property of CASE-B is its ability to control nose-up pitching moment effectively. The pitching moment generation for the short (DDF) CASE-B is very much suppressed when compared to tall (DDF) CASE-A. CASE-B nose-up pitching moments are about the same as the values predicted for the baseline duct. The short (DDF) concept described in Figure 6.b is a highly effective scheme of improving the lip separation related inlet flow distortion problem for the rotor of a ducted fan based VTOL/STOL vehicle. CASE-B is able to improve thrust without increasing the nose-up pitching moment generation. Since the leading side of the fan exit jet is well balanced against the trailing side of the exit jet, the effectiveness of the control surfaces at the exit of the ducted fan are expected to function much effectively for the short (DDF) CASE-B.

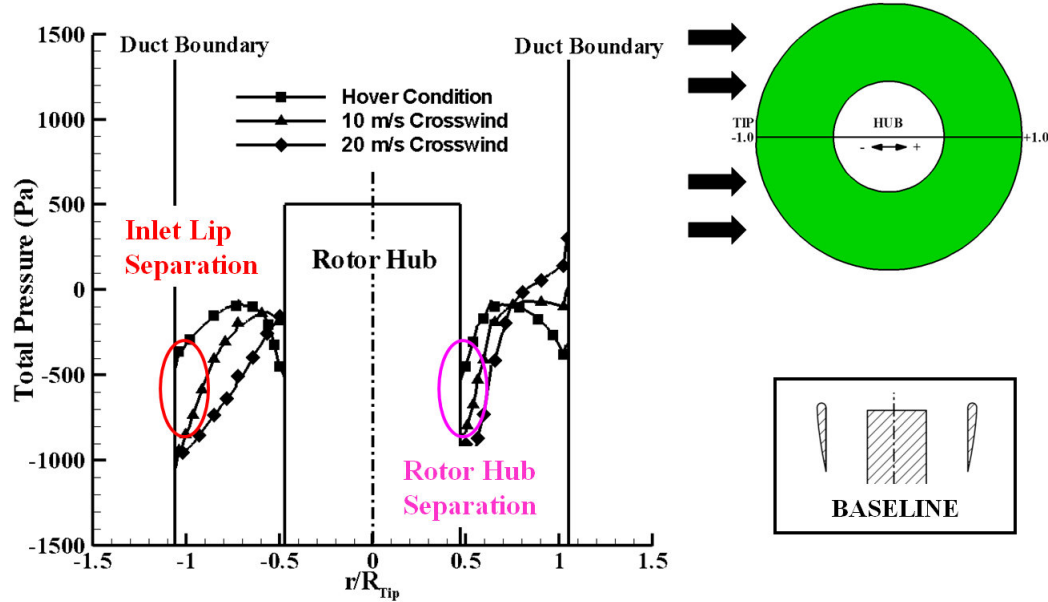


Figure 4.3: Rotor inlet total pressure deficit at elevated forward flight speed for the baseline ducted fan $P_{t,inlet}@10m/s = 61.25 \text{ pa}$, $P_{t,inlet}@20m/s = 245 \text{ pa}$

Figure 4.3 shows the total pressure obtained 1mm upstream of the base-line ducted fan rotor for hover, and two forward flight velocities. The spanwise total pressure distribution between the duct leading edge and trailing edge for hover condition shows a relatively flat total pressure distribution at the inlet surface. The inlet field is symmetrical between the leading side and trailing side along a radial line passing from the axis of rotation.

When the baseline ducted fan increases its forward flight speed to 10 m/s, a very visible inlet total pressure defect due to leading side lip separation is apparent as shown by the green symbols in Figure 10. At 20 m/s forward flight speed, the total pressure defect near the leading side of the duct is significantly increased (blue symbols). The low momentum fluid entering the leading side of the rotor occupies a much wider portion of the blade span.

The trailing side of the rotor shows a very different inlet total pressure distribution along the flight direction as shown in Figure 4.3. The inlet flow passing over the inlet plane tends to stagnate on the trailing side of the baseline duct aft surface (shroud) due to the specific orientation of inlet streamlines in this region, especially at elevated forward flight velocities. The triangular and diamond symbols representing 10 m/s and 20 m/s forward flight velocities show the elevated levels of total pressure near the trailing side of the duct inner surface. This type of total pressure augmentation only occurring during forward flight is directly related to an unwanted drag force acting in opposite direction to forward flight direction.

Figure 4.3 also reveals another local flow separation zone in the trailing side of the baseline duct inlet surface. The inlet flow progressing to enter into the trailing portion of the duct also separates from the the rotor hub surface, generating a low momentum zone as shown in Figure 4.3.

Figure 4.3 clearly shows the imbalance between the leading side and trailing side of the duct inlet flow field in terms of local total pressure. The duct has tremendous air breathing difficulty near the leading side of the duct. Due to blocked nature of the leading side flow, the trailing side sees an inlet flow with an unnecessarily elevated level of total pressure near the shroud surface. However there is a significant total pressure deficit near the hub surface for forward flight conditions due to rotor hub corner separation.

The short double ducted fan (DDF) CASE-B has an ability to control the inlet lip separation leading to improved thrust and well controlled nose-

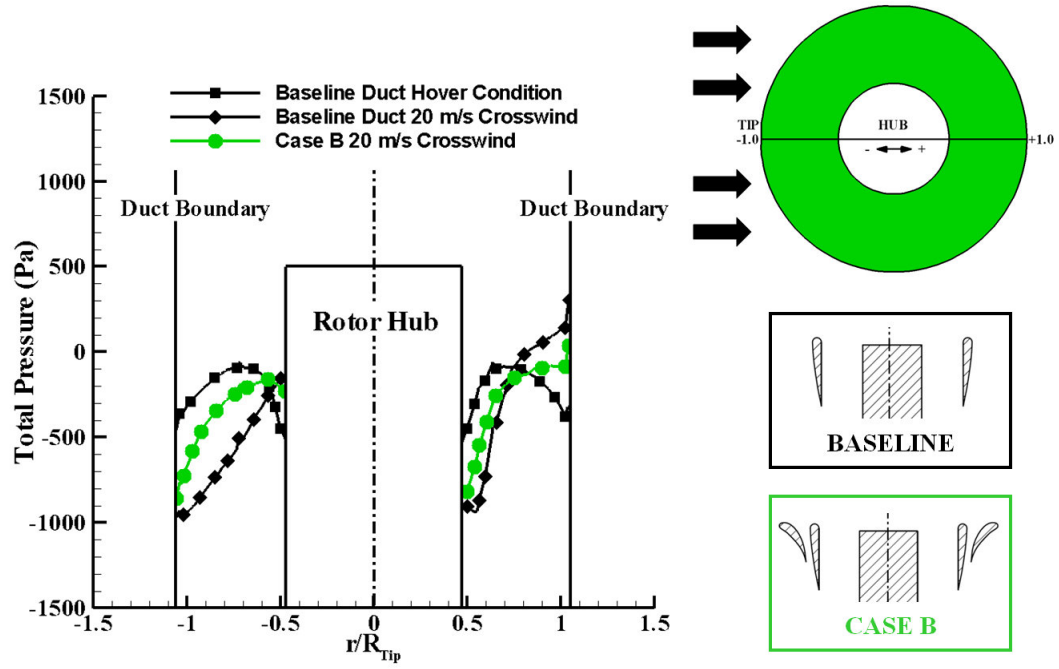


Figure 4.4: Reduction in rotor inlet flow distortion between the leading side and trailing side of (DDF) CASE-B short double ducted fan
 $P_{t,inlet@20m/s} = 245 \text{ pa}$

up pitching moment. Figure 4.4 shows the lip separation improvements of CASE-B in comparison to the baseline duct. The black square symbols define the rotor inlet total pressure distribution in spanwise direction for the baseline fan under hover conditions. The inlet flow under hover conditions does not have any significant inlet flow distortion for the baseline ducted fan.

Inlet flow character of the baseline ducted fan in horizontal flight is represented by the black diamond symbols for the forward flight speed of 20 m/s. The green circular symbol shows the inlet total pressure distribution generated by the short double ducted fan (DDF) CASE-B. The inlet lip separation related total pressure deficit of the baseline configuration is effectively reduced by the use of the short double-ducted fan (DDF) CASE-B (green circular symbols in Figure 4.4). The local mass flow rate passing

from the leading side of the duct is much improved because of the short double-ducted fan (DDF) CASE-B. The unnecessarily elevated total pressure observed near the aft shroud of the baseline ducted fan (trailing side) as shown by black diamond symbols is also controlled when CASE-B is implemented (green circular symbols). This reduction of total pressure on the trailing side of (DDF) CASE-B is beneficial in balancing the leading side and trailing side flow of the fan rotor exit flow field. CASE-B also reduces drag generation occurring near the aft part of the shroud.

4.3 A Comparative Evaluation of Local Velocity Magnitude, Streamlines and Total Pressure for All Three Ducts

As part of the (DDF) concept validation, local flow field details including magnitude of velocity, streamlines and total pressure distributions are presented over a surface passing through the duct leading edge, axis of rotation and the trailing edge of the duct system. Comparisons of the specific (DDF) design against the corresponding baseline duct at 9000 rpm are discussed using the computational predictions explained in the previous paragraphs. The baseline duct; Case-A, the tall DDF; and CASE-B, the short DDF results are compared in detail.

4.3.1 CASE-A Tall (DDF) versus Baseline Duct Results /at 10 m/s and 20 m/s

Figure 4.5 compares the flow fields of tall double ducted fan designated as CASE-A and the baseline duct. A slight forward lip separation is observed at 10 m/s forward flight velocity. The tall double ducted fan CASE-A produces an enhanced thrust level of 1.73 times that of the baseline ducted fan at 10 m/s. The mass flow rate of CASE-A at 9000 rpm is also enhanced when compared to the baseline ducted fan, as shown in Figure 4.5. The total pressure distributions clearly show the low momentum regions due to inlet lip separation and hub corner separation on the rotor disk inlet surface as shown by dark blue areas in Figure 4.5. The tall ducted fan provides a reduction in the size of the low momentum flow areas downstream of the inlet lip and hub corner when compared to the baseline duct.

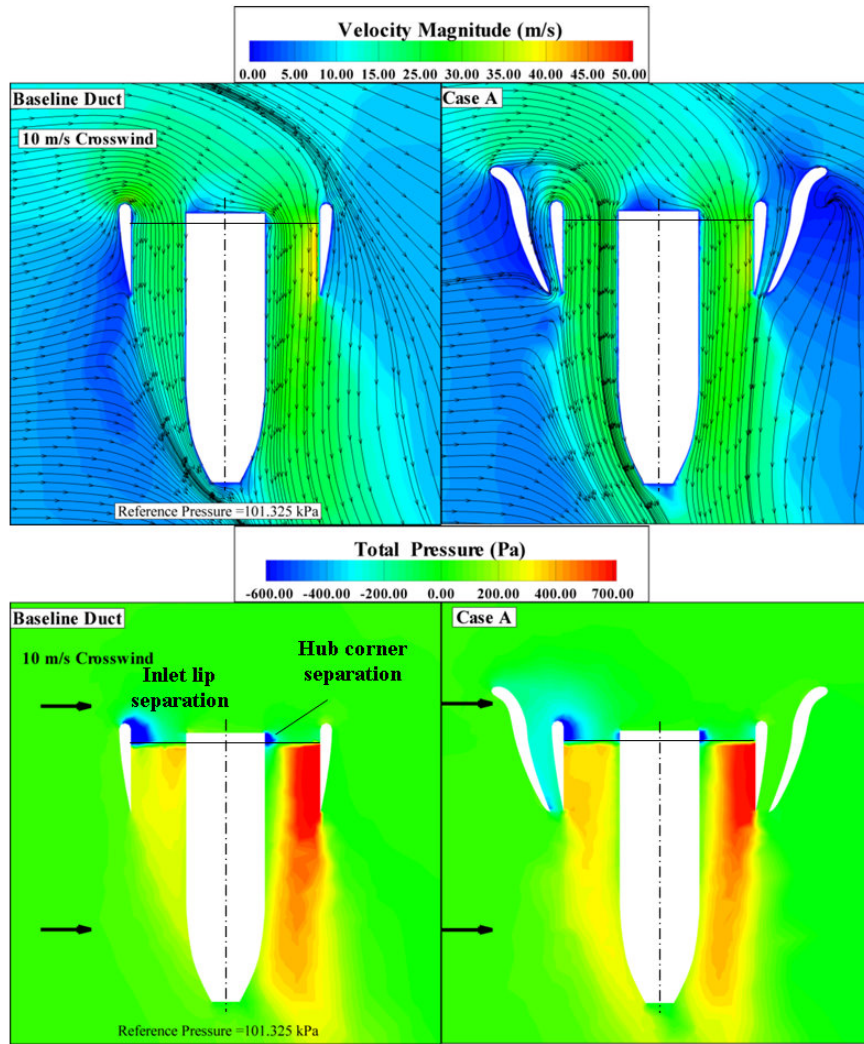


Figure 4.5: Velocity magnitude and total pressure distribution,baseline duct versus CASE-A tall double ducted fan (DDF) at 10 m/s forward flight velocity

Although the “*hub corner separation*” area is relatively smaller than the “*inlet lip separation*” area, the flow blockage created by the hub corner separation affects the flow downstream of the rotor as shown in Figure 4.5. The total pressure imbalance observed at downstream of the rotor for the baseline duct is significant. The existence of the tall double ducted fan

CASE-A slightly improves the total pressure on the leading side of the rotor exit flow for 10 m/s forward flight velocity.

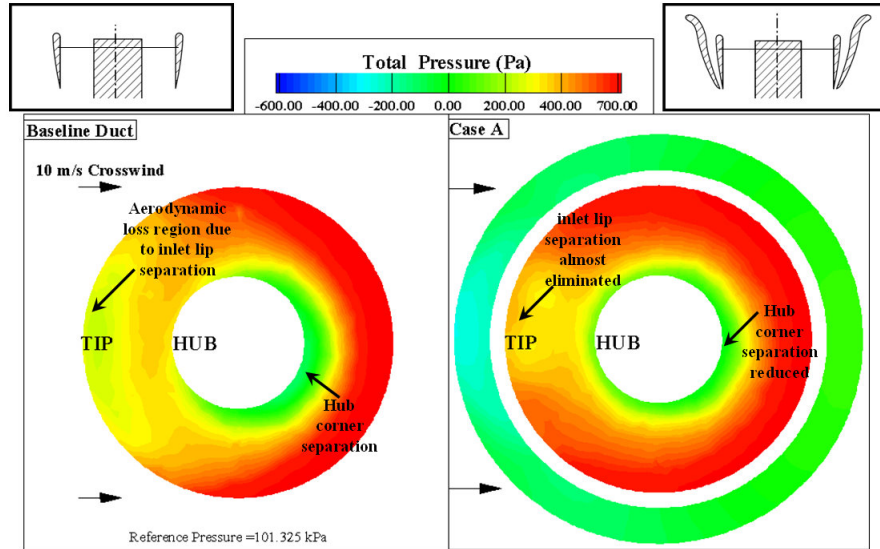


Figure 4.6: Total pressure distribution at rotor exit plane (horizontal) baseline duct versus CASE-A tall double ducted fan (DDF) at 10 m/s forward flight velocity

Figure 4.6 explains the effect of inlet flow distortion existing in the baseline duct and tall double ducted fan design at 10 m/s forward flight velocity by using rotor exit total pressure predictions. The light green zone near the leading side of the baseline ducted fan shows the highest level of aerodynamic loss resulting from “*inlet lip separation*” at 10 m/s. This area is where the relative flow tends to separate because of the existence of the duct lip near the leading side. The fan inlet surface also has another aerodynamic loss region (green) at just downstream of the “*hub corner*” on the trailing side of the duct. The beneficial influence of the tall double ducted fan design CASE-A is shown in Figure 4.6. The aerodynamic loss areas in the baseline duct distribution are effectively reduced in the tall double ducted fan design. The red total pressure zone near the trailing side of the baseline duct shows the highest levels of total pressure over the rotor exit plane. The trailing side tends to pass most of the inlet mass flow rate including the fluid that

is skipping over (deflected by) the lip separation region. This is a common observation in most standard ducted fans in horizontal flight.

The aft part of the fan usually generates additional drag force because of this red high total pressure zone at the exit plane. The implementation of the tall double ducted fan makes the total pressure distortion between the leading side and trailing side much more balanced. The inlet flow distortion is efficiently dealt with with the implementation of the second duct configuration termed as CASE-A, Figure 4.6.

When forward flight velocity is increased to 20 m/s, Figure 4.7 shows the highly adverse character of the separated flow zone behind the inlet lip section in the baseline duct. The flow also tends to separate behind the hub corner on the trailing side of the duct. Figure 4.7 demonstrates that the flow is nearly blocked by the existence of a large separated flow zone and the flow is effectively induced into the trailing side of the duct. The imbalance in the local mass flow rate between the leading side of the duct and the trailing side of the duct at 20 m/s is much more apparent when compared to 10 m/s results. Figure 4.7 displays the significant flow improvement in the lip separation area for the tall double ducted fan (DDF) CASE-A. The re-circulatory flow is almost eliminated downstream of the lip. The leading side of the duct starts breathing effectively because of CASE-A's ability to eliminate inlet flow distortion near the leading side. The (DDF) CASE-A results show a low momentum region that could be viewed as a three dimensional wake region behind the vehicle at 20 m/s forward flight velocity. The outer duct flow near the leading side is in a direction opposite to rotor flow direction. The outer duct flow near the leading side is an essential component of the (DDF) concept because of its highly important role in reversing the inner lip region separated flow conditions. The outer duct flow smoothly reverses into the rotor flow direction away from the leading side.

The rotor exit plane total pressure distribution shown in Figure 4.8, (DDF) CASE-A reveals a significant lip separation improvement leading to a much uniform inlet flow distribution between the leading side and trailing side of the inner duct. The DDF duct local flow distribution at the rotor exit is much improved in comparison to the baseline duct. Hub corner separation area is also reduced in (DDF) CASE-A. Most circumferential positions of the second duct (other than the leading side of the duct) contributes to the generation of thrust because of the measurable outer duct flow observed in

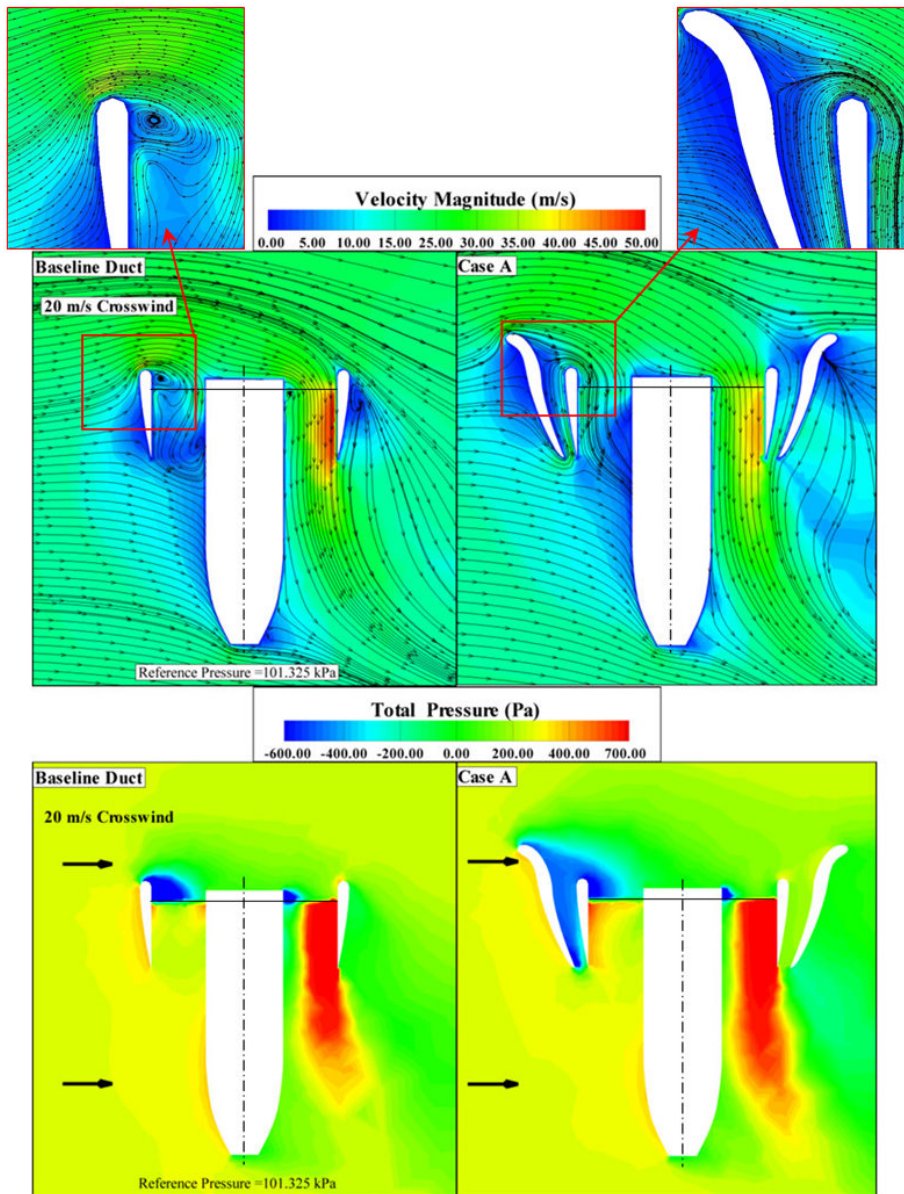


Figure 4.7: Velocity magnitude and total pressure distribution, baseline duct versus CASE-A tall double ducted fan (DDF) at 20 m/s forward flight velocity

this area.

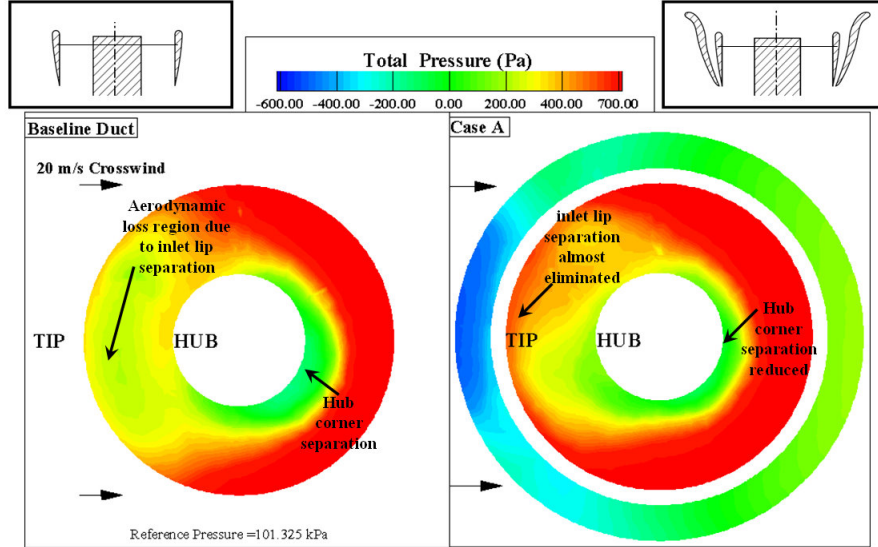


Figure 4.8: Total pressure distribution at rotor exit plane (horizontal) baseline duct versus CASE-A tall double ducted fan (DDF) at 20 m/s forward flight velocity

4.3.2 CASE-B Short (DDF) versus Baseline Duct Results at 10 m/s and 20 m/s

Figures 4.9 and 4.10 show the most effective double ducted fan (DDF) treatment results obtained for a forward flight velocity of 10 m/s. A detailed geometrical definition of the short double ducted fan (DDF) CASE-B was discussed in Figure 2.2b.

The short DDF has the ability to improve thrust in relative to the baseline case “*without producing a significant nose-up pitching moment*” by effectively reducing inlet lip separation and hub corner separation areas. The short double ducted fan configuration is a self adjusting lip separation control system preserving its separation control features in a wide range of forward flight velocities. The effectiveness of the short DDF treatment is shown in the total pressure distribution presented in Figure 4.9 for 10 m/s flight velocity. In addition to the area reduction of the separated flow areas (dark blue), the total pressure imbalance between the leading side and

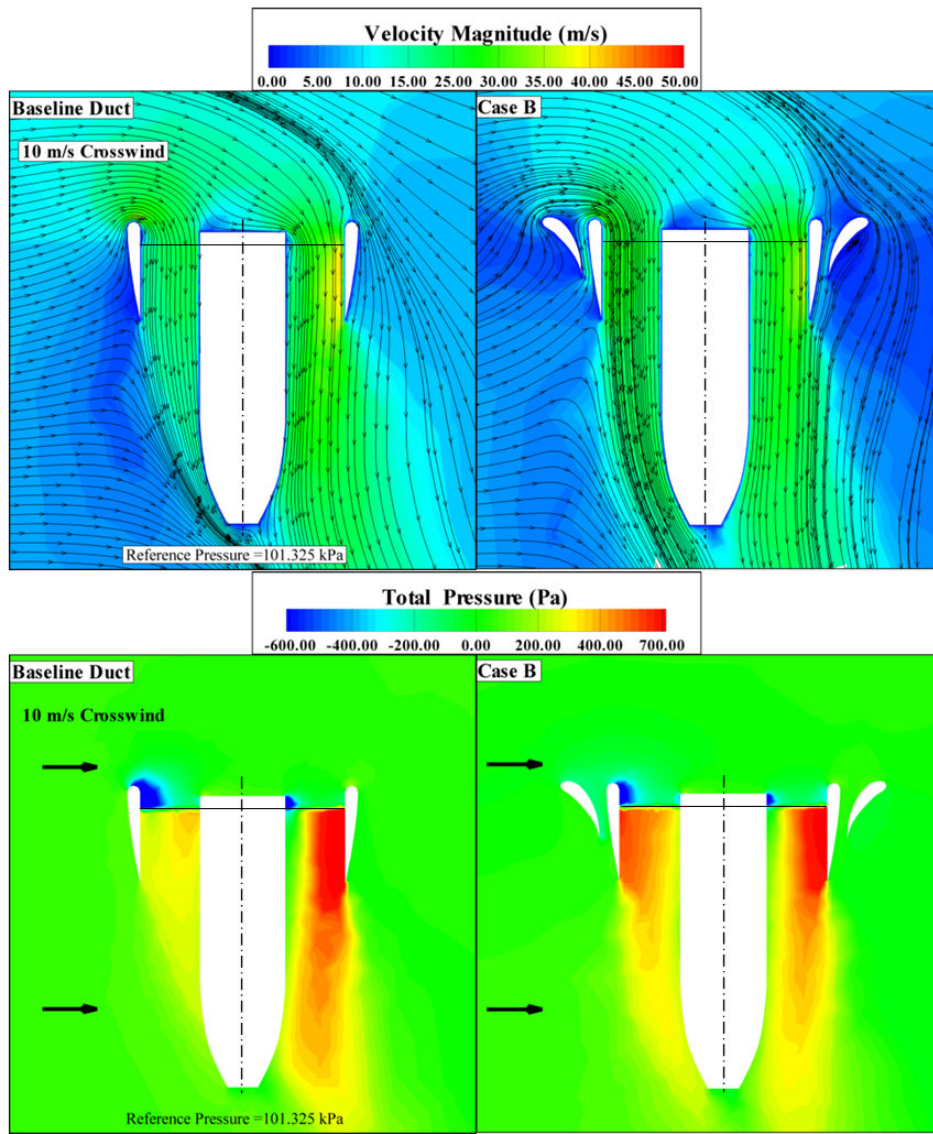


Figure 4.9: Velocity Magnitude and total pressure distribution, baseline duct versus CASE-B short double ducted fan (DDF) at 10 m/s forward flight velocity

trailing side is almost eliminated. The leading side of the inner duct of the short DDF CASE-B breathes at a much improved rate as compared to the baseline case. The red high total pressure areas provide a well-balanced fan

exit jet near the leading side and trailing side of the fan.

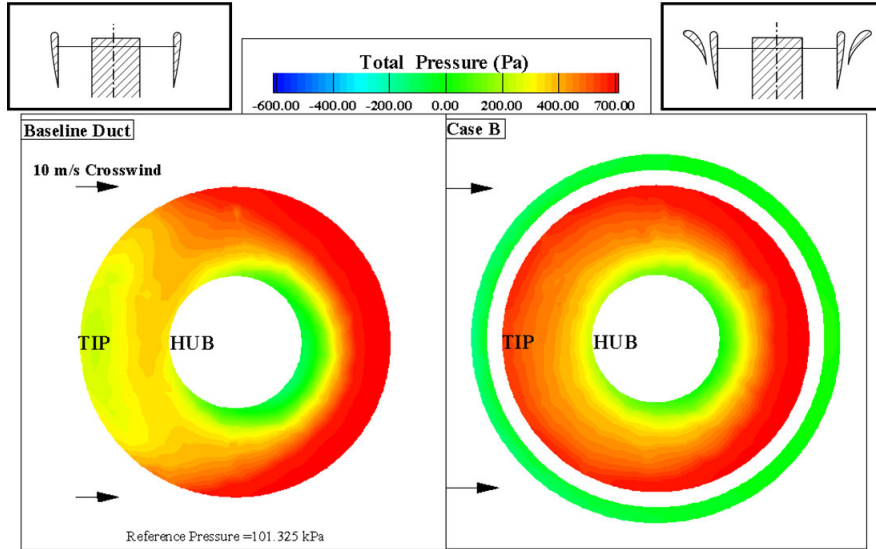


Figure 4.10: Total pressure distribution at rotor exit plane (horizontal) baseline duct versus CASE-B short double ducted fan (DDF) at 10 m/s forward flight velocity

Figure 4.10 indicates a high level of rotor exit total pressure uniformity for CASE-B in contrast to the strong flow distortion generated by the baseline duct. When short double ducted fan is used, the lip separation and hub corner separation control is highly effective at 10 m/s flight velocity. The level of total pressure values between the leading side and trailing side are much better balanced in CASE-B as shown in Figure 4.10.

When the short double ducted fan arrangement (DDF) CASE-B is evaluated at 20 m/s flight velocity, the loss elimination features near the leading side lip, hub corner area are much apparent. Highly separated lip region flow adversely blocking the leading side of the inner duct is successfully dealt with the flow control features of the short (DDF) as shown in Figure 4.11. A well-balanced short (DDF) exit flow provides a higher level of thrust when compared to the baseline duct. The flow improvements and thrust enhancement from the short (DDF) comes with no additional nose-up pitching

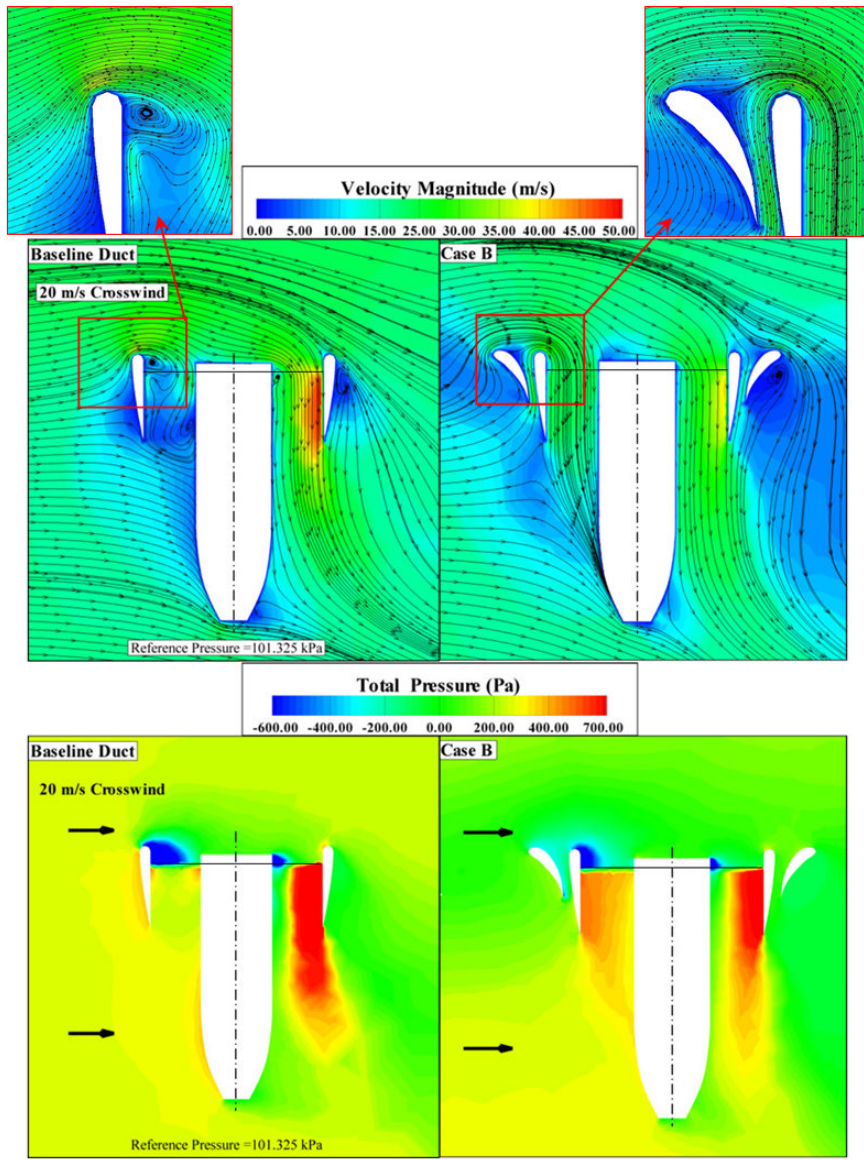


Figure 4.11: Velocity magnitude and total pressure distribution, baseline duct versus CASE-B short double ducted fan (DDF) at 20 m/s forward flight velocity

moment generation when compared to baseline as explained in Table 4.2

and Figure 4.11. A highly effective inlet flow distortion control ability of the short ducted fan can be apparently seen in Figure 4.12. A vehicle using the short (DDF) concept CASE-B generates a higher level of thrust with a well balanced ducted fan exit flow without excessive generation of nose-up pitching moment. This approach results in improvements of the performance of the control surfaces and improved range because the energy efficiency of the ducted fan is improved. The elimination of severe inlet flow distortion is likely to improve the rotor exit flow quality before further interaction with typical control surfaces.

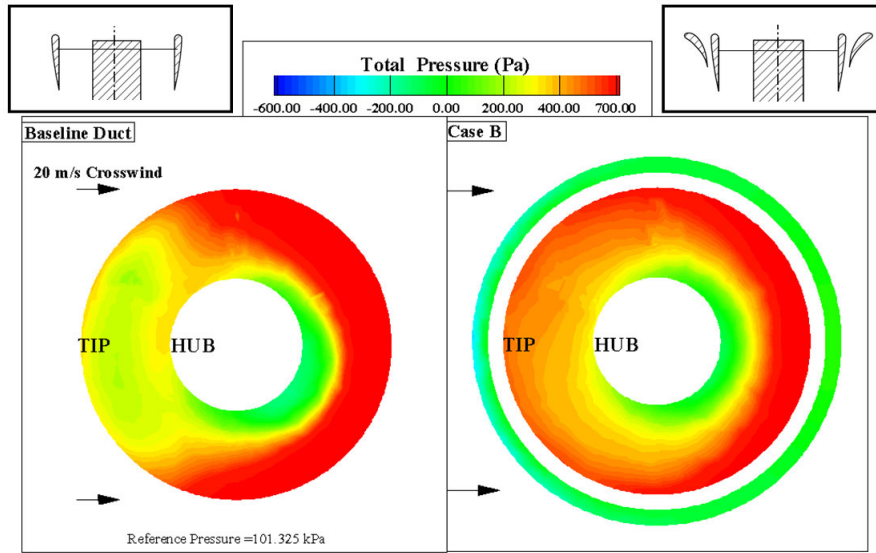


Figure 4.12: Total pressure distribution at rotor exit plane (horizontal) baseline duct versus CASE-B short double ducted fan (DDF) at 20 m/s forward flight velocity

4.4 Upstream Lip Region Local Flow Improvements in (DDF)

Figure 4.13 defines the local sampling locations for static pressure and skin friction coefficient computations on the airfoil of the inner duct at the leading

edge location. The lowercase characters represent the “*rotor side*” locations and the uppercase characters show the “*outer side*” sampling locations for static pressure and skin friction coefficient on the inner duct airfoil section. The “*outer side*” denotes the channel between the baseline duct and secondary duct.

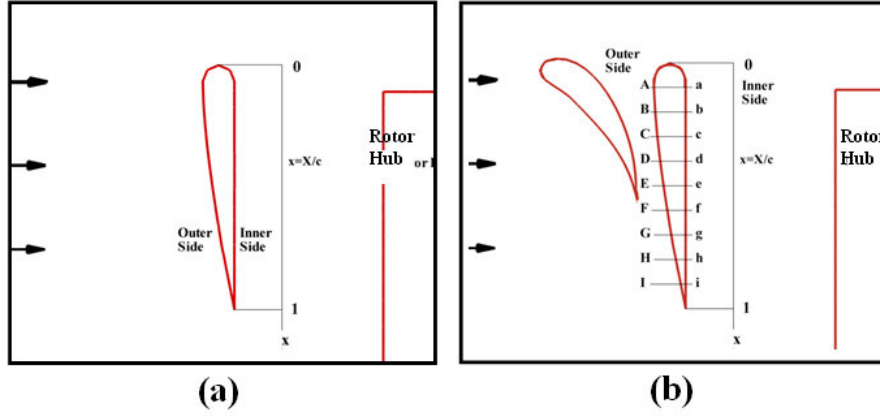


Figure 4.13: Sampling locations for static pressure and skin friction coefficient computations near the leading side of the inner duct for (DDF) CASE-B

4.4.1 Static Pressure Distribution around the Lip Section of the Baseline Duct

Figure 4.14 shows the static pressure distribution for the baseline duct and double ducted fan (DDF) CASE-B for the forward flight velocity of 20 m/s. The distributions presented in Figure 4.14 are plotted around the airfoil of the baseline duct. The pressure gradient occurring around the leading edge radius of the inner duct is the most significant parameter controlling severeness of the leading edge lip separation problem. Point $x=X/c=0$ shows the leading edge and $x=X/c=1$ shows the trailing edge location of the baseline duct airfoil. The external flow stagnates on the the baseline duct airfoil at point D as shown in Figure 4.14 . The approaching flow to the duct is divided into a stream reaching up to the leading edge and a second stream approaching down to the trailing edge of the duct airfoil at point D. The static (or stagnation) pressure from point D to J remains almost constant. The external flow slightly accelerates to the leading edge

point from point C to A for the baseline duct. There is a strong acceleration zone between point A and the leading edge point O, as clearly shown by the favorable pressure gradient between the point A and O. This is the area within the leading edge diameter of the inner lip section. The geometrical leading edge point O is the minimum pressure point for the baseline duct airfoil. The flow on the inner side of the lip sees a very strong adverse pressure gradient around the leading edge circle. The strong flow separation character shown in Figure 4.14 is mainly due to the strong adverse pressure gradient affecting the boundary layer growth between points O, a and finally b. The rotor process described in equations from 3.1 to 3.6 results in the sudden pressure rise on the inner part of the baseline duct between b and c.

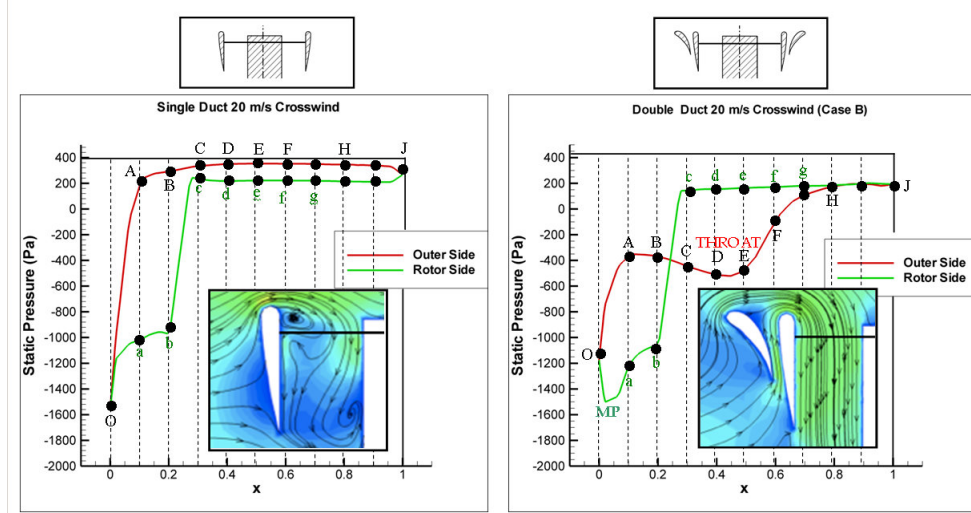


Figure 4.14: Comparison of the static pressure distribution on the baseline lip section and inner duct lip section of the (DDF) CASE-B airfoil

4.4.2 Static Pressure Distribution around the Lip section of the Double Ducted Fan (DDF)

Figure 4.14 also shows the static pressure distribution around the lip section of the short double ducted fan (DDF) CASE-B. The vertically upward channel flow in the outer duct section is established by the dynamic pressure of the external flow in forward flight. The vertically upward flow exists in a narrow leading edge region as clearly shown in Figure 4.11 and the results

showing the axial velocity vectors from the computations. The outer duct flow that is proceeding vertically up generates a unique wall static pressure distribution in a converging-diverging channel. The external flow in horizontal flight stagnates on the shorter outer airfoil and turns upward towards the leading edge of the outer duct airfoil. Most of the flow stagnating at the lower part of the vehicle is directed towards the converging diverging channel of the outer duct. There is a wide stagnation region between points J and H on the outer side of the inner duct. The flow accelerates towards the throat section of the outer duct near D. The flow after the throat section smoothly decelerates up to the point A that is very close to the leading edge circle of the leading edge. The existence of the diverging channel is responsible from a much softer acceleration around the leading edge diameter of the lip section between A and O. The flow is still accelerating when it is passing through the geometrical leading edge point O. The minimum pressure point (MP) in (DDF) configuration is on the inner side of the lip section at $x=X/c=0.03$ in contrary to the baseline duct location O. The flow starts decelerating after this minimum pressure point MP. The adverse pressure gradient region after the minimum pressure point MP in (DDF) is much shorter and the adverse pressure gradient between MP and a is much milder than that of the baseline duct. Figure 4.14 clearly shows the favorable modified nature of the static pressure distribution around the lip section of (DDF) leading to the elimination of the severe inlet lip separation region that is unique to the baseline duct in forward flight. The (DDF) approach is extremely useful in controlling the inner lip flow separation originating the adverse pressure gradient region.

4.4.3 Skin Friction Distribution around the Leading Edge of the Duct

Figure 4.15 presents the skin friction coefficient distributions on the baseline duct lip section and inner duct lip section of the (DDF) configuration. The skin friction coefficient c_f is defined as the local wall shear stress normalized by inlet dynamic head defined as the lowest level of the predicted wall shear stress is on the lip surface along the separated flow region for the baseline duct. This low momentum region is between points O and a corresponding to the highest level of adverse pressure gradients before the rotor inlet plane. The overall level of wall shear stress is higher between points a and b for the double duct configuration showing the immediate influence of weakened adverse pressure gradients resulting from the (DDF) geometry. The DDF

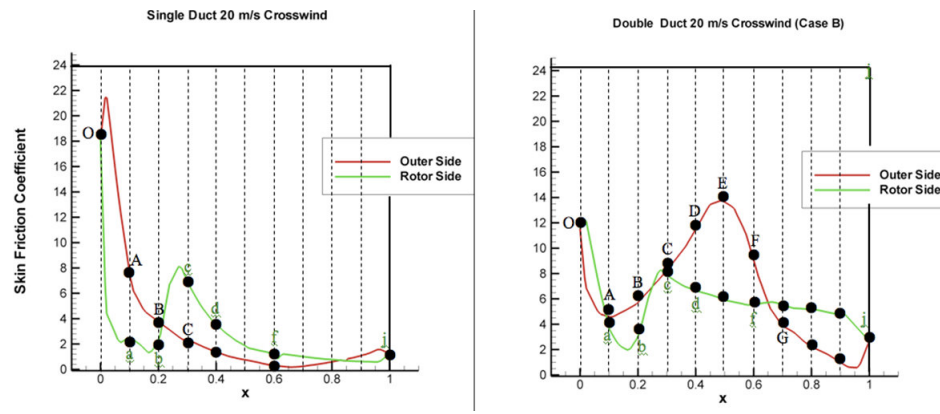


Figure 4.15: Comparison of the skin friction coefficient distribution on the baseline lip section and inner duct lip section of the (DDF) airfoil

geometry significantly reduces the aerodynamic shear stress occurring near the inner lip of the DDF system especially near the leading edge.

Chapter 5

Conclusions

This technical paper describes a novel ducted fan inlet flow conditioning concept that will significantly improve the performance and controllability of VTOL “vertical take-off and landing” vehicles, UAVs “uninhabited aerial vehicles” and many other ducted fan based systems. The new (DDF) concept developed in this study deals with most of the significant technical problems in ducted fans operating at almost 90° angle of attach, in the edge-wise flight mode. The technical problems related to this mode of operation are as follows:

- Increased aerodynamic losses and temporal instability of the fan rotor flow when “*inlet flow distortion*” from “*the lip separation area*” finds its way into the tip clearance gap leading to the loss of energy addition capability of the rotor.
- Reduced thrust generation from the upstream side of the duct due to the rotor breathing low-momentum re-circulatory turbulent flow.
- A severe imbalance of the duct inner static pressure field resulting from low momentum fluid entering into the rotor on the leading side and high momentum fluid unnecessarily energized on the trailing side of the rotor.
- A measurable increase in power demand and fuel consumption when the lip separation occurs to keep up with a given operational task.
- Lip separation and its interaction with the tip gap flow requires a much more complex vehicle control system because of the severe non-uniformity of the exit jet in circumferential direction and excessive pitch-up moment generation.

- At low horizontal speeds a severe limitation in the rate of descent and vehicle controllability may occur because of more pronounced lip separation. Low power requirement of a typical descent results in a lower disk loading and more pronounced lip separation.
- Excessive noise and vibration from the rotor working with a significant inlet flow distortion.
- Very complex unsteady interactions of duct exit flow with control surfaces.

The new concept that will significantly reduce the inlet lip separation related performance penalties in the edgewise flight zone is named “*DOUBLE DUCTED FAN (DDF)*”. The current concept development uses a time efficient 3D computational viscous flow solution approach developed specifically for ducted fan flows. The present study summarizes only the most optimal approach after evaluating nine different double ducted fan geometries for a wide range of edgewise flight velocities.

The current concept uses a secondary stationary duct system to control “*inlet lip separation*” related momentum deficit at the inlet of the fan rotor occurring at elevated edgewise flight velocities. The DDF is self-adjusting in a wide edgewise flight velocity regime.

DDFs corrective aerodynamic influence becomes more pronounced with increasing flight velocity due to its inherent design properties.

Case-B was the best DDF configuration designed. It has improved mass flow rate passing from the duct by 40 % and improved thrust force obtained from the ducted fan by 56.2 % relative to baseline duct in edgewise flight condition.

The DDF can also be implemented as a “*Variable Double Ducted Fan*” (VDDF) for a much more effective inlet lip separation control in a wide range of horizontal flight velocities in UAVs, air vehicles, trains, buses, marine vehicles and any axial flow fan system where there is significant lip separation distorting the inlet flow.

Most axial flow fans are designed for an inlet flow with zero or minimal inlet flow distortion. The DDF concept is proven to be an effective way of dealing with inlet flow distortions occurring near the tip section of any axial flow fan rotor system operating at high angle of attack.

Bibliography

- [1] Abrego, A. I. and Bulaga, R. W., 2002, "Performance study of a ducted fan system," AHS Aerodynamics, Aeroacoustic , Test and Evaluation Technical Specialist Meeting.
- [2] Martin, P. and Tung, C., 2004, "Performance and flowfield measurements on a 10-inch ducted rotor vtol uav," 60th Annual Forum of the American Helicopter Society.
- [3] Fleming, J., Jones, T., Lusardi, J., Gelhausen, P., and Enns, D., 2004, "Improved control of ducted fan vtol uavs in crosswind turbulence," AHS 4th Decennial Specialist's Conference on Aeromechanics.
- [4] Moller, P. S., 1989, "Robotic or remotely controlled flying platform," U.S. Patent No: 4795111.
- [5] Graf, W., Fleming, J., and Wing, N., 2008, "Improving ducted fan uav aerodynamics in forward flight," 46th AIAA Aerospace Sciences Meeting and Exhibit.
- [6] Graf, W. E., 2005, *Effects of Duct Lip Shaping and Various Control Devices on the Hover and Forward Flight Performance of Ducted Fan UAVs*, Master's thesis, Virginia Polytechnic Institute and State University, Blacksburg, Virginia.
- [7] Lazareff, M., 2008, "Improving ducted fan uav aerodynamics in forward flight," 46th AIAA Aerospace Sciences Meeting and Exhibit.
- [8] Van Weelden, S. D., Smith, D. E., and Mullins, B. R., Jr., 1996, "Preliminary design of a ducted fan propulsion system for general aviation aircraft," AIAA 34th Aerospace Sciences Meeting and Exhibit.
- [9] Kriebel, A. R. and Mendehall, M. R., 1966, "Predicted and measured performance of two full-scale ducted propellers," CAL/USA AVLabs

Symposium on Aerodynamic Problems Associated with V/STOL Aircraft, Vol II: Propulsion and Interference Aerodynamics.

- [10] Mort, K. W. and Gamse, B., 1967, "A wind tunnel investigation of a 7-foot-diameter ducted propeller," Tech. Rep. NASA TND-4142.
- [11] Mort, K. W. and Yaggy, P. F., 1962, "Aerodynamic characteristics of a 4-foot-diameter ducted fan mounted on the tip of a semispan wing," Tech. Rep. NASA TND-1301.
- [12] Yaggy, P. F. and Mort, K. W., 1961, "A wind-tunnel investigation of a 4-foot-diameter ducted fan mounted on the tip of a semispan wing," Tech. Rep. NASA TND-776.
- [13] Weir, R. J., 1988, "Aerodynamic design consideration for a free flying ducted propeller," AIAA Atmospheric Flight Mechanics Conference.
- [14] Pereira, J. L., 2008, *Hover and Wind-tunnel Testing of Shrouded Rotors for Improved Micro Air Vehicle Design*, Ph.D. thesis, University of Maryland, Maryland.
- [15] Martin, P. B. and Boxwell, D. A., 2005, "Design, analysis and experiments on a 10-inch ducted rotor vtol uav," AHS International Specialists Meeting on Unmanned Rotorcraft: Design, Control and Testing.
- [16] Lind, R., Nathman, J. K., and Gilchrist, I., 2006, "Ducted rotor performance calculations and comparisons with experimental data," 44th AIAA Aerospace Sciences Meeting and Exhibit.
- [17] He, C. and Xin, H., 2006, "An unsteady ducted fan model for rotorcraft flight simulation," 62th AHS Forum.
- [18] Chang, I. C. and Rajagopalan, R. G., 2003, "Cfd analysis for ducted fans with validation," 21th AIAA Applied Aerodynamics Conference.
- [19] Ahn, J. and Lee, K. T., 2004, "Performance prediction and design of a ducted fan system," 40th AIAA/ASME/SAE/ASEE Joint Propulsion Conference and Exhibit.
- [20] Ko, A., Ohanian, O. J., and Gelhausen, P., 2007, "Ducted fan uav modeling and simulation in preliminary design," AIAA Modeling and Simulation Technologies Conference and Exhibit.
- [21] Zhao, H. W. and Bil, C., 2008, "Aerodynamic design and analysis of a vtol ducted-fan uav," 26th AIAA Applied Aerodynamics Conference.

- [22] Dorman, H. A. and Dorman, B. A., 1960, "Aircraft having a plurality of annular wings," U.S. Patent No: 2951661.
- [23] Bright, C. E., 1961, "Ducted fan aircraft," U.S. Patent No: 2968453.
- [24] Yoeli, R., 2002, "Ducted fan vehicles particularly useful as vtol aircraft," U.S. Patent No: 6464166.
- [25] Piasecki, F. N., 1965, "Flying platform," U.S. Patent No: 3184183.
- [26] Fletcher, C. I., 1961, "Ducted fan aircraft," U.S. Patent No: 2988301.
- [27] Boyd, E. S., Mallory, M., and Skinner, L. R., 1970, "Vertical takeoff and landing aircraft," U.S. Patent No: 3519224.
- [28] Wen, L., 1977, "Vertical takeoff and landing aircraft," U.S. Patent No: 4049218.
- [29] Cycon, J. P., Rosen, K. M., and Whyte, A. C., 1992, "Unmanned flight vehicle including counter rotating rotors positioned within toroidal shroud and operable to provide all required vehicle flight control," U.S. Patent No: 5152478.
- [30] Moffit, R. C. and Owen, S. J., 1992, "Shroud geometry for unmanned aerial vehicles," U.S. Patent No: 5150857.
- [31] Flemming, R. J., Rosen, K. M., and Sheehy, T. W., 1995, "Ancillary aerodynamic structures for an unmanned aerial vehicle having ducted, coaxial counter-rotating rotors," U.S. Patent No: 5419513.
- [32] Swinson, J., Walker, S., and James, T. J., 1999, "Horizontal and vertical take off and landing unmanned aerial vehicle," U.S. Patent No: 5890441.
- [33] Cycon, J. P., Scott, M. W., and DeWitt, C. W., 2001, "Method of reducing a nose-up pitching moment on a ducted unmanned aerial vehicle," U.S. Patent No: 6170778.
- [34] Cycon, J. P., Scott, M. W., and DeWitt, C. W., 2001, "Unmanned aerial vehicle with counter-rotating ducted rotors and shrouded pusher-prop," U.S. Patent No: 6270038.
- [35] Moller, P. S., 2002, "Stabilizing control apparatus for robotic or remotely controlled flying platform," U.S. Patent No: 6450445.

- [36] Wagner, J., Pruszenski, A., and Milde, K. F., 2005, "Vtol personal aircraft," U.S. Patent No: 6886776.
- [37] Yoeli, R., 2005, "Vehicles particularly useful as vtol vehicles," U.S. Patent No: 6883748.
- [38] Yoeli, R., 2007, "Ducted fan vtol vehicles," U.S. Patent No: 2007/0034739.
- [39] Yoeli, R., 2007, "Ducted fan vehicles particularly useful as vtol aircraft," U.S. Patent No: 7275712.
- [40] ANSYS, 2009, "Anssys-fluent v12 user's guide," .
- [41] Akturk, A., 2010, *Ducted Fan Inlet/Exit and Rotor Tip Flow Improvements for Vertical Lift Systems*, Ph.D. thesis, The Pennsylvania State University, Pennsylvania.